WIND transcription factors orchestrate wound-induced callus formation, vascular reconnection and defense response in Arabidopsis

Iwase, Akira ; Kondo, Yuki ; Laohavisit, Anuphon ; Takebayashi, Arika ; Ikeuchi, Momoko ; Matsuoka, Keita ; Asahina, Masashi ; Mitsuda,···

(URL)
https://hdl.handle.net/20.500.14094/0100476500

WIND transcription factors orchestrate wound-induced callus formation, vascular reconnection and defense response in Arabidopsis

Akira Iwase[1,2] (iD), Yuki Kondo[3,4] (iD), Anuphon Laohavisit[1] (iD), Arika Takebayashi[1], Momoko Ikeuchi[1,5] (iD), Keita Matsuoka[6], Masashi Asahina[6,7] (iD), Nobutaka Mitsuda[8] (iD), Ken Shirasu[1,3] (iD), Hiroo Fukuda[3] (iD) and Keiko Sugimoto[1,3] (iD)

[1]RIKEN Center for Sustainable Resource Science, Yokohama 230-0045, Japan; [2]JST, PRESTO, Kawaguchi 332-0012, Japan; [3]Department of Biological Sciences, Graduate School of Science, The University of Tokyo, Bunkyo-ku, Tokyo 113-0033, Japan; [4]Department of Biology, Graduate School of Science, Kobe University, Kobe 657-8501, Japan; [5]Department of Biology, Faculty of Science, Niigata University, 8050 Ikarashi 2-no-cho, Nishi-ku, Niigata, Japan; [6]Department of Biosciences, Teikyo University, 1-1 Toyosatodai, Utsunomiya 320-8551, Japan; [7]Advanced Instrumental Analysis Center, Teikyo University, 1-1 Toyosatodai, Utsunomiya 320-8551, Japan; [8]Bioproduction Research Institute, National Institute of Advanced Industrial Science and Technology (AIST), Tsukuba 305-8566, Japan

Summary

• Wounding triggers *de novo* organogenesis, vascular reconnection and defense response but how wound stress evoke such a diverse array of physiological responses remains unknown.

• We previously identified AP2/ERF transcription factors, WOUND INDUCED DEDIFFERENTIATION1 (WIND1) and its homologs, WIND2, WIND3 and WIND4, as key regulators of wound-induced cellular reprogramming in Arabidopsis. To understand how WIND transcription factors promote downstream events, we performed time-course transcriptome analyses after *WIND1* induction.

• We observed a significant overlap between WIND1-induced genes and genes implicated in cellular reprogramming, vascular formation and pathogen response. We demonstrated that WIND transcription factors induce several reprogramming genes to promote callus formation at wound sites. We, in addition, showed that WIND transcription factors promote tracheary element formation, vascular reconnection and resistance to *Pseudomonas syringae* pv. tomato DC3000.

• These results indicate that WIND transcription factors function as key regulators of wound-induced responses by promoting dynamic transcriptional alterations. This study provides deeper mechanistic insights into how plants control multiple physiological responses after wounding.

Introduction

Wounding is a serious threat to the plant survival and it triggers multiple physiological responses to quickly heal and protect damaged tissues from pathogen invasion (Reymond *et al.*, 2000; Cheong *et al.*, 2002). In plants, formation of a pluripotent cell mass, called callus, at wound sites is often a key step to regenerate new organs and develop physical and chemical barriers against pathogens (Birnbaum & Alvarado, 2008; Asahina *et al.*, 2011; Ikeuchi *et al.*, 2013, 2016; Melnyk, 2017). Importantly, wounding and callus formation is often accompanied by vascular reformation presumably to establish the route for water and nutrient transport in developing cell mass (Fukuda, 1997; Mazur *et al.*, 2016). Accordingly, earlier studies reported ectopic tracheary element formation in the genetic tumor of *Nicotiana tabacum* callus

(White, 1939) and crown galls (Van Lith-Vroom *et al.*, 1960). It is also known that grafted plants initially form callus at wound sites, followed by vascular bundle reformation within callus (Melnyk *et al.*, 2015; Melnyk, 2017). Surface regeneration of debarked tree trunk is another well-characterized regeneration phenomenon after wounding where xylem and phloem reformation occur after callus formation (Stobbe *et al.*, 2002). Although we have made considerable progress in our understanding of how plants perceive wounding signals (Toyota *et al.*, 2018; Ikeuchi *et al.*, 2019, 2020; Marhava *et al.*, 2019), our knowledge on how plants initiate such a diverse array of wound-induced responses is still very limited (Bloch, 1941; Walker-Simmons *et al.*, 1984; Savatin *et al.*, 2014).

Given that these wound-induced events require dynamic changes in gene expression, it is likely that plants possess some

transcriptional mechanisms to coordinate their progression. Recent studies have indeed identified several wound-inducible transcription factors that have critical roles in regeneration (Ikeuchi et al., 2013, 2016, 2019; Xu & Huang, 2014). We previously reported that an APETALA2/ETHYLANE RESPONSE FACTOR (AP2/ERF) transcription factor WOUND INDUCED DEDIFFERENTIATION 1 (WIND1) and its close homologs, WIND2, WIND3 and WIND4, promote wound-induced callus formation through activating the cytokinin response (Iwase et al., 2011a,b, 2013, 2015). WIND1 also promotes shoot regeneration via direct activation of another AP2/ERF transcription factor *ENHANCER OF SHOOT REGENERATION 1* (*ESR1*) (Iwase *et al.*, 2017, 2018). WIND induction, in addition, leads to somatic embryogenesis on phytohormone-free medium (Ikeuchi *et al.*, 2013), implying that WIND1 can drive multiple developmental pathways to promote regeneration. At the cellular level, WIND1 promotes the acquisition of regenerative competence since ectopic overexpression of *WIND1* can bypass wounding and early incubation steps on auxin-rich callus inducing medium (CIM), which are the prerequisite for shoot regeneration on cytokinin-rich shoot inducing medium (SIM) (Valvekens et al., 1988; Iwase et al., 2015). Several other AP2/ERF family transcription factors are also implicated in the control of regeneration since PLETHORA3 (PLT3), PLT5 and PLT7, are critical for wound-induced callus formation and pluripotency acquisition under CIM/SIM condition (Kareem *et al.*, 2015; Ikeuchi *et al.*, 2017, 2020). Another wound-inducible AP2/ERF protein ETHYLENE RESPONSE FACTOR 115 (ERF115), acting upstream of *WIND1*, is required for reformation of root stem cells and regeneration of root meristems after injury (Heyman et al., 2013, 2016; Marhava et al., 2019; Zhou et al., 2019). ERF113/RELATED TO AP2 6 LIKE (RAP2.6L), which is a close homolog of ERF115, is reported as a key regulator of tissue reconnection process (Asahina *et al.*, 2011) as well as for shoot regeneration under CIM/SIM condition (Che et al., 2006).

Several important transcriptional regulators of plant vascular development have also been identified (Kondo, 2018) and for instance, VASCULAR-RELATED NAC-DOMAIN6 (VND6) and VND7 transcription factors function as master regulators for the formation of vascular vessels (Kubo et al., 2005). Overexpression of *VND6* or *VND7* provokes ectopic tracheary element formation in diverse cell types (Kubo et al., 2005). LATERAL ORGAN BOUNDARIES DOMAIN 30 (LBD30), a putative positive feedback regulator for *VND6* and *VND7*, also shows similar ectopic tracheary formation when overexpressed in *Arabidopsis thaliana* (Arabidopsis) (Soyano *et al.*, 2008). Other Arabidopsis NAC domain transcription factors ANAC071 and ANAC091 are required in tissue reconnection and conversion of mesophyll cell fate to cambial cells (Asahina *et al.*, 2011; Matsuoka *et al.*, 2021). Recent studies using the *in vivo* and *in vitro* culturing system have started to unveil further transcriptional regulatory networks driving the vascular development (Kondo et al., 2016; Miyashima et al., 2019). When Arabidopsis leaf tissues are incubated under the Vascular Cell Induction Culture System Using Arabidopsis Leaves (VISUAL), leaf mesophyll cells

reprogram into vascular cells and start to express cambium cell marker genes such as *TDIF RECEPTOR* (*TDR*) and *Arabidopsis thaliana HOMEOBOX GENE8* (*AtHB8*) (Kondo *et al.*, 2016). This is followed by the upregulation of xylem marker genes, such as *IRREGULAR XYLEM3* (*IRX3*), and phloem marker genes such as *SIEVE-ELEMENT-OCCLUSION-RELATED*1 (*SEOR1*). Despite these progresses, whether these key regulators contribute to xylem formation after wounding and if so, how wounding activates these regulators remain unknown.

Hierarchal transcriptional networks acting from pathogen perception to the immune responses (Cui et al., 2015) are well characterized and many WRKY transcription factors are known to play major roles in defense signaling (Eulgem & Somssich, 2007). WRKY18 and WRKY53, for instance, positively regulate defense responses and these regulators induce genes for key enzymes in biosynthesis of phytoalexins, the antimicrobial secondary metabolites (Wang *et al.*, 2006; Murray *et al.*, 2007). Camalexin, a well-known phytoalexin in Arabidopsis, is synthesized *de novo* after various biotic and abiotic stress including pathogen infection (Ahuja *et al.*, 2012). P450 monooxygenases, Cytochrome P450 71B15 (CYP71B15/PAD3) and CYP71A13, are involved in camalexin biosynthesis and they are induced after pathogen infection in a WRKY33-dependent manner (Qiu *et al.*, 2008). A single knock-out mutation of these P450 monooxygenases enhances disease susceptibility against bacterial pathogen infection (Rajniak *et al.*, 2015).

Lysine-derived pipecolic acid is a critical regulator for an establishment of systemic acquired resistance in *Arabidopsis* upon pathogen infection, and is synthesized via AGD2-LIKE DEFENSE REPONSE PROTEIN 1 (ALD1) (Hartmann et al., 2018). *ALD1* also shows WRKY33-dependent expression manner, and importantly, plants defective in this gene show higher susceptibility to pathogens (Song *et al.*, 2004; Návarová *et al.*, 2012; Wang *et al.*, 2018), indicating that the control of WRKY-mediated phytoalexin and signal molecule production are crucial for the defense response.

Interestingly, ERF108/RELATED TO AP2 6 (RAP2.6), a close homolog of ERF115 and RAP2.6L in the subfamily X of AP2/ERF transcription factors, may function in the defense response since its expression is strongly induced after challenged with a virulent *Pseudomonas syringae* pv. tomato DC3000 (*Pst* DC3000). ERF108/RAP2.6 also promotes resistance against cyst nematode infection though the enhancement of callose deposition in *Arabidopsis* (He *et al.*, 2004; Ali *et al.*, 2013). These findings highlight the multifaceted roles of AP2/ERF transcription factors in tissue repair and defense responses (Heyman *et al.*, 2018) but how their stress-induced expression is regulated remains to be elucidated.

Several recent transcriptome studies revealed that the wound-induced transcriptional changes highly overlap with those elicited by various biotic and abiotic stresses (Cheong et al., 2002; Ikeuchi et al., 2017; Melnyk et al., 2018), suggesting the existence of common regulators that function in multiple stress responses. Given that callus produced by constitutive *WIND1* expression shows increased expression of some vascular genes and defense response genes (Iwase *et al.*, 2011a), it is plausible that WIND1 and its

homologs play diverse roles in response to wounding and other forms of stress. In this study we conducted the time-course transcriptome analyses after *WIND1* induction to explore how WIND1 functions in stress response. Our data show that WIND1 transcriptionally activates over 2000 genes implicated in cellular reprogramming, vascular formation and defense response. Further functional analyses confirmed that WIND transcription factors have important roles during wound-induced cellular reprogramming, vascular regeneration and defense response. Our results, therefore, provide important molecular insights into how plants coordinately control regeneration and innate immunity through WIND-mediated transcriptional mechanisms.

Materials and Methods

Plant materials, growth condition, and transformation

All Arabidopsis plants used in this study were in the Col-0 background. *XVE-WIND1*, *WIND1pro:WIND1-SRDX*, *wind1* (SALK_020767 and SALK_027272), *wind2* (SALK_139727), *wind3* (SALK_091212), *wind4* (SALK_099481), *wind1 wind2 wind3 wind4* quadruple mutant (generated by crossing *wind* single mutants), *rap2.6l-1* (SALK_051006), *rap2.6-1* (GK_053G11.01), *rap2.6-3* (SAIL_1225_G09), *35S:RAP2.6-1*, *35S:RAP2.6-2*, *erf115* (SALK_021981), *ERF115pro:ERF115-SRDX*, *plt3 plt5 plt7* triple mutant, *wox5-1* (SALK_038262), and *anac071 anac096 anac011* were described previously (Che *et al.*, 2006; Sarkar *et al.*, 2007; Iwase *et al.*, 2011a; Ali *et al.*, 2013; Heyman *et al.*, 2013; Kareem *et al.*, 2015; Ikeuchi *et al.*, 2017; Matsuoka *et al.*, 2018; Matsuoka *et al.*, 2021). T-DNA insertion lines were obtained from the Arabidopsis Biological Resource Center (ABRC). Plants were grown on 0.6% (w/v) gelzan plates containing Murashige & Skoog (MS) salt and 1% sucrose medium at 22°C with a photoperiod of 16 h white light and 8 h darkness, unless noted otherwise. For plant transformation, T-DNA vectors carrying an appropriate construct were introduced into *Agrobacterium tumefaciens* strain GV3101 by electroporation, and Arabidopsis plants were transformed by the floral dip method (Clough & Bent, 1998). For *WIND*1 induction, 10-d-old wild-type (WT) plants and XVE-WIND1 plants were grown on MS plates, which were treated with MS liquid medium containing either mock control or 10 μM 17-β-estradiol (ED; Sigma-Aldrich, St Louis, MO, USA).

Plasmid construction

To construct the *Pro_{RAP2.6L}:RAP2.6L-GFP* and *Pro_{RAP2.6L}:RAP2.6L-SRDX* vectors, genomic fragments containing the 2000-bp promoter sequence and coding sequence were amplified by PCR and cloned between SpeI and SmaI sites of *pGFP_NOSG* (Iwase *et al.*, 2017) and *pSRDX_NOSG* vectors (Yoshida *et al.*, 2013), respectively. The resulting *Pro_{RAP2.6L}:RAP2.6L-GFP* and *Pro_{RAP2.6L}:RAP2.6L-SRDX* fragments were subcloned into the *pBCKH* vector (Mitsuda *et al.*, 2006) by Gateway LR Clonase II (Thermo Fisher Scientific, Waltham, MA, USA) and used for plant transformation. To construct the *Pro:L-*

LUC reporter vectors, the 3000-bp promoter sequence of each gene (At1g05100, At1g09950, At3g50260, At4g28140, At4g38400 and At1g02460) was amplified by PCR and cloned between ApaI or SacII and NotI sites of the *ProESR1:LUC* vector (Iwase *et al.*, 2017). A list of primers used for PCR amplification is provided in Supporting Information Table S5.

Transient expression assay

The *Pro_{35S}:WIND1* (Iwase *et al.*, 2011a) and *Pro_{35S}:SG* (Ohta *et al.*, 2001) vectors were used as an effector and control, respectively. The *Pro:L-LUC* vectors were used as reporters, and the *pPTRL* vector which drives the expression of a luciferase gene from Renilla (R-LUC) by the 35S promoter (Fujimoto *et al.*, 2000), was used as an internal control. Particle bombardment and luciferase assays were performed as described previously (Iwase *et al.*, 2017).

RNA isolation, microarray and RT-qPCR analyses

Total RNA was isolated with RNeasy Plant Mini Kit (Qiagen, Vemlo, the Netherlands) according to manufacturer's instruction. Microarray experiments were performed using Agilent Arabidopsis (V3) (4x44k) microarray according to the manufactures' instruction. Four biological replicates were tested in one-color method. Spot signal values were calculated by FEATURE EXTRACTION v.9.1 software supplied by Agilent Technologies (Santa Clara, CA, USA). The quality control (QC) values were defined as one when a spot passes the 'FeatNonUnifOL' filter and as two when the spot further passes the 'FeatPopnOL' filter. Detection values were defined as one when a spot passes the 'IsPosAndSignif' filter and as two when the spot further passes the 'IsWellAboveBG'. Global normalization among different replicates and experiments were performed with quantile normalization method (Amaratunga & Cabrera, 2001) by using > 100 our in-house same-platform data followed by division of each value by the median value among spots with QC = 2. Spot-to-gene conversion was accomplished based on a table provided by TAIR (ftp://ftp.arabidopsis.org/home/tair/Microarrays/Agilent/agilent_array_elements-2009-7-29.txt). The average values were used for the genes corresponding to two or more probes. Genes with average QC value < 1.5 in the 'test' sample or the 'reference' sample were excluded from further analyses, and only genes with average detection value ≥ 1.5 in the 'test' or 'reference' sample were analyzed when selecting for upregulated or downregulated genes. The P values of each gene were calculated by Welch's *t*-test. To estimate the false discovery rate (FDR), Q-value was calculated from P value, using the QVALUE software (default settings; (Storey & Tibshirani, 2003)), and upregulated or downregulated (> 2-fold or < 0.5-fold) genes were selected with P value less than 0.05 (FDR was less than 0.05 in each case). Binomial test was performed by R (http://www.r-project.org/). Hierarchical clustering analysis was performed using the CLUSTER 3 software, using default settings (Eisen *et al.*, 1998; de Hoon *et al.*, 2004). Reverse transcription quantitative polymerase chain reaction (RT-qPCR) was performed as described previously (Mitsuda *et al.*, 2005).

Mean expression levels were normalized against the *PROTEIN PHOSPHATASE 2A SUBUNIT A3* (*PP2AA3*) gene. The transcriptome data were deposited in the National Center for Biotechnology Information (NCBI) Gene Expression Omnibus as GSE167174 (https://www.ncbi.nlm.nih.gov/geo/query/acc.cgi?acc=GSE167174;token=slwleqkextstbon).

Callus formation and vascular induction assay

Callus formation assay from petioles was performed as described previously (Iwase *et al.*, 2017). To induce tracheary element formation in cotyledons, VISUAL (Kondo *et al.*, 2016) was employed using whole seedlings without cut treatment. The rate of tracheary element formation was evaluated by BF-170 (Sigma-Aldrich) staining according to a previous study (Nurani *et al.*, 2020).

Petiole grafting assay

The middle part of the first and second leaf petioles of 16-d-old plants was transversely cut by razor blade (FA-10; Feather, Osaka, Japan) and grafted together in a silicon tube with 0.5 mm diameter (As One, Osaka, Japan). After incubating the grafted plants at 22°C under continuous light for 12 d, their roots were soaked in water containing 1 mM 5-CFDA florescent dye (Cosmo Bio, Tokyo, Japan) for 1 h. Xylem reformation at wound sites was judged by dissection microscope and the transmission of fluorescent dyes into grafted leaf vasculature was used as criteria for successful grafting. Physical reconnection at graft sites was assessed by pulling leaf blades apart after the xylem formation check. Tracheary elements in graft junction were stained with phloroglucinol reagent (1% (w/v) phloroglucinol (Fujifilm Wako, Osaka, Japan) in 20% (v/v) hydrochloric acid) for 10 min under vacuum at room temperature. Stained samples were mounted in chloral hydrate solution (8 g chloral hydrate (Fujifilm Wako), 1 ml glycerol (Fujifilm Wako) and 2 ml deionized water) before microscopy.

Microscopy

Callus and BF-170 signals were observed under Leica M165 C stereomicroscope. Propidium iodide signals, autofluorescence and phloroglucinol signals from secondary cell walls were visualized by a Leica TCP SP5 II confocal laser microscope and BX51 microscope (Olympus).

Pathogen infection assay

The pathogenic bacterial growth assays were performed as described previously (Laohavisit *et al.*, 2020), with slight modification. Plants for pathotest were grown in a mixture of vermiculite and soil (1 : 1) under short day conditions (8 h : 16 h, light : dark, 21°C : 22°C) for 5–6 wk. *Pseudomonas syringae* pv. tomato (*Pst*) DC3000 were grown in liquid King's B medium at 28°C before experiment. Leaves of different *Arabidopsis* lines were inoculated with the virulent bacterial pathogen either by infiltration.

Bacterial suspension (optical density at 600 nm (OD_{600nm}) = 0.0002) were syringe infiltrated into the leaves of 5- to 6-wk-old plants. Plants were maintained at high humidity during the course of infection and returned to the same growth regime (8 h : 16 h, light : dark, 21°C : 22°C). Leaf discs were taken 3 d post-inoculation (day 3) from three leaves per plant, with six plants per genotype per independent trial. Bacterial growth was assessed by colony counting.

Accession numbers

Sequence data from this article can be found in the Arabidopsis Genome Initiative under the following accession numbers: *PP2AA3* (At1g13320), *WIND1* (At1g78080), *WIND2* (At1g22190), *WIND3* (At1g36060), *WIND4* (At5g65130), *PLT3* (At5g10510), *PLT5* (At5g57390), *PLT7* (At5g65510), *ERF115* (At5g07310), *RAP2.6L* (At5g13330), *RAP2.6* (At1g43160), *VND6* (At5g62380), *VND7* (At1g71930), *LBD30* (At4g00220), *WOX5* (At3g11260), *ANAC071* (At4g17980), *ANAC096* (At5g46590), *ANAC011* (At1g32510), *WRKY18* (At4g31800), *WRKY40* (At1g80840), *WRKY53* (At4g23810), *CYP71A13* (At2g30770), *ALD1* (AT2G13810), *MAPKKK18* (At1g05100), *RAS1* (At1g09950), *DEAR1* (At3g50260), *ERF54* (At4g28140), *ATEXPL2* (At4g38400) and a gene cording pectin lyase-like superfamily protein (At1g02460).

Results

WIND1 induction causes dynamic transcriptional changes with distinct temporal expression patterns

To understand the gene expression dynamics after *WIND1* induction, we performed time-course transcriptome analyses using *XVE-WIND1* plants where we induced *WIND1* expression by the application of ED (Supporting Information Fig. S1a). We harvested WT and *XVE-WIND1* plants at 1, 3, 6, 12 and 24 h after ED treatment and confirmed the induction of *WIND1* transcript level by RT-qPCR analysis in the ED-treated *XVE-WIND1* seedlings (Fig. S1b). We subsequently searched for differentially expressed genes (DEGs) between ED- and dimethyl sulfoxide (DMSO)-treated *XVE-WIND1* seedlings by the microarray analysis and identified 2390 genes that were more than two-fold upregulated and 2140 genes that were more than two-fold downregulated in at least one time point after *WIND1* induction (FDR < 0.05) (Tables S1 and S2). We observed an increase in the number of DEGs over the 24 h time course (Fig. S1c), implying the existence of gene regulatory networks governed by WIND1. Since WIND1 functions primarily as a transcriptional activator (Iwase *et al.*, 2017), we decided to focus on the 2390 upregulated genes and subjected them to the k-means clustering analysis. These upregulated genes can be grouped in four different classes according to their temporal expression patterns (Fig. 1a). Class I included 274 genes that showed early and transient induction, given their expression was upregulated at 1 and/or 3 h after induction, and reverted back to the basal level by 6 h. By contrast, 728 genes in class II showed

upregulation at 1 or 3 h after WIND1 induction and their expression remained high within the 24 h time period. Classes III and IV included 721 genes which were upregulated at 6 h, and 667 genes which were upregulated at 12 h, respectively, after

WIND1 induction. Since *WIND1* was expressed constitutively in this experimental system (Fig. S1b; Table S1), the majority of its downstream genes remained highly expressed once they were induced. The transient nature of class I gene expression, however,
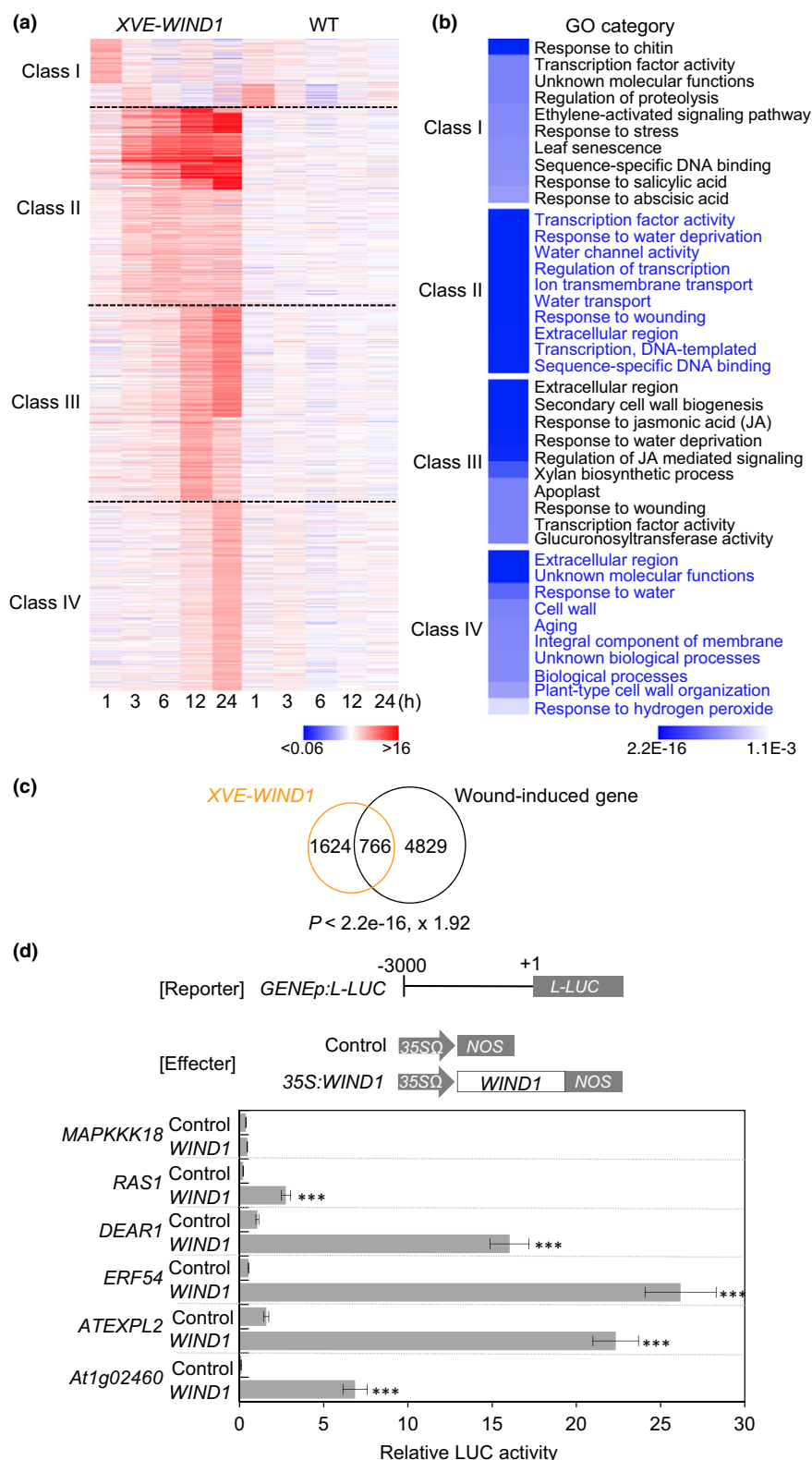
Fig. 1 WIND1 induces gene expression with distinct temporal patterns. (a) Heat-map representation of WIND1-induced transcriptional changes. Gene expression at 1, 3, 6, 12, 24 h after 17β-estradiol (ED) treatment is shown for *XVE-WIND1* and wild-type (WT) seedlings. Values are fold change relative to dimethyl sulfoxide (DMSO)-treated seedlings. WIND1-induced genes can be grouped into four classes by k-means clustering analysis. Class I contains 274 genes that are transiently expressed within 1 or 3 h after WIND1 induction. Class II includes 728 genes that are constitutively expressed after WIND1 activation. The 721 genes in Class III and 667 genes in Class IV are expressed from 12 and 24 h, respectively, after WIND1 induction. (b) Gene ontology (GO) analysis for classes I–IV genes. GO categories such as response to chitin and transcription factor activity are over-represented among class I genes. GO categories such as transcription factor activity and response to wounding are over-represented among class II genes. GO categories such as extracellular region and secondary cell wall biogenesis are over-represented among classes III and IV genes. The *P*-values are shown in color codes for each GO category. (c) Venn diagram showing the overlap between WIND1-induced genes in *XVE-WIND1* plants and genes induced by wounding in Arabidopsis hypocotyls (Ikeuchi *et al.*, 2017). The significance of overlap between a pair of gene sets is evaluated by Fisher's exact test, and *P*-values and odds ratio are shown. (d) Transient activation of putative WIND1 target genes in Arabidopsis culture cells. Upper panel shows the reporter construct, *GENEp:L-LUC*, and effector constructs, control and *35S:WIND1*, used in the transient activation analysis. The black bar in the reporter construct represents the 3000-bp promoter sequence of putative downstream genes. The gray box represents the coding sequence of L-LUC, encoding a firefly luciferase gene, and +1 ATG indicates the translational start site. For the effector constructs, gray arrows mark *35SΩ*, the cauliflower mosaic virus 35S promoter with the tobacco mosaic virus omega translation amplification sequence, and gray boxes mark NOS, the *Agrobacterium tumefaciens* nopaline synthase transcriptional terminator. The white box marks the *WIND1* coding sequence. Bottom panel shows the promoter activity of six putative WIND1 target genes as judged by the L-LUC activity relative to R-LUC, *Renilla* luciferase. Cobombardment of *35S:WIND1* and *GENEp:L-LUC* shows the transactivation of target promoter by WIND1. Data are mean ± SE (*n* = 6, technical replicates). Statistical significance is determined by Student *t*-test (***, *P* < 0.001).

inferred that their expression was tightly regulated by negative feedback mechanisms.

Gene ontology (GO) analysis for class I genes revealed that GO categories such as 'response to chitin' (*P* value = 1.66E-08, odds ratio = 10.29) were over-represented (Fig. 1b). Since chitin is implicated in defense signaling (Kaku *et al.*, 2006), this enrichment suggests that WIND1 activates defense responses. The GO term 'transcription factor activity' (*P* value = 5.63E-06, odds ratio = 2.36) was also highly ranked (Fig. 1b), strongly suggesting that WIND1 primarily targets transcriptional regulators. The GO category 'transcription factor activity' (*P* value = 7.44E-14, odds ratio = 2.40) was also ranked as the top category among class II genes, reinforcing the idea that WIND1 functions as a key regulator of transcriptional network. As expected, we also found 'response to wounding' (*P* value = 8.08 E-09, odds ratio = 4.77) in class II as well as in class III (*P* value = 1.26 E-05, odds ratio = 3.67), confirming that majority of wound-responsive genes are WIND1-inducible (Cheong *et al.*, 2002; Delessert *et al.*, 2004; Iwase *et al.*, 2011a). In addition, 'Response to water deprivation' was over-represented among class II (*P* value = 7.98 E-11, odds ratio = 4.55) and class III (*P* value = 1.09E-07, odds ratio = 3.77) genes, supporting the notion that water deprivation may contribute to the expression of wound-induced genes (Reymond *et al.*, 2000). Furthermore, GO terms such as 'extracellular region' (*P* value = 2.20E-16, odds ratio = 2.20), 'secondary cell wall biogenesis' (*P* value = 8.46E-10, odds ratio = 11.89) and 'xylan biosynthetic process' (*P* value = 2.56E-06, odds ratio = 12.08) were over-represented among class III genes, suggesting that cell wall remodeling may be initiated within 12 h after *WIND1* induction. Enrichment of a GO term 'glucuronosyltransferase activity' (*P* value = 2.18E-05, odds ratio = 15.53) from class III genes also supported such an idea since genes, such as *GLUCURONIC ACID SUBSTITUTION OF XYLAN1* (*GUX1*) and *GUX2* (Table S1) which encode xylan glucuronosyltransferases required for the remodeling of cell wall polysaccharides, hemicelluloses (Rennie *et al.*, 2012), were included in this category. It is also worth noting that other GO terms such as

'response to jasmonic acid (JA)' (*P* value = 4.54E-09, odds ratio = 5.49) and 'regulation of JA-mediated signaling pathway' (*P* value = 3.11E-07, odds ratio = 12.85) were also over-represented among class III genes, implying that WIND1 activates long-term JA responses. Among class IV genes, 'extracellular region' was the most highly ranked GO term and several other terms such as 'cell wall' and 'plant-type cell wall organization' were also over-represented, suggesting that WIND1 promotes cell wall reorganization beyond 24 h. Among 11 genes representing the 'response to water' category (*P* value = 3.41E-06, odds ratio = 22.89), 5 out of 10 dehydrin genes in Arabidopsis (Hanin *et al.*, 2011) were upregulated (Table S1), predicting that WIND1 may participate in the dehydration tolerance. Enrichment of 'unknown molecular functions' (*P* value = 2.25E-08, odds ratio = 1.43) is intriguing and could reflect unclarified physiological responses driven by WIND1. These data together suggest that *WIND1* activation triggers a series of cellular and physiological processes ranging from the early defense response to the later, more prolonged dehydration response and rearrangement of cell wall polysaccharides.

We have previously shown that wound stress upregulates 5595 genes within 24 h in Arabidopsis hypocotyls (Ikeuchi *et al.*, 2017). Comparison between these wound-induced genes and 2390 WIND1-induced genes revealed that 32.1% of WIND1-induced genes (766 genes out of 2390 genes, *P* value = 2.2E-16, odds ratio = 1.92) were also induced by wounding (Fig. 1c), further substantiating an important role of WIND1 as the key transcriptional activator in response to wounding. To further confirm that WIND1 acts as a transcriptional activator for wound-induced genes, we randomly selected the following six genes from the list of 766 genes, including *MITOGEN ACTIVATED PROTEIN KINASE KINASE KINASE 18* (*MAPKKK18*), *RESPONSE TO ABA AND SALT 1* (*RAS1*), *DREB AND EAR MOTIF PROTEIN 1* (*DEAR1*), *ERF54*, *ARABIDOPSIS THALIANA EXPANSIN LIKE 2* (*ATEXPL2*) and *At1g02460/*pectin lyase-like superfamily protein, that were induced by both WIND1 induction and wounding (Fig. 1c; Table S1) and tested
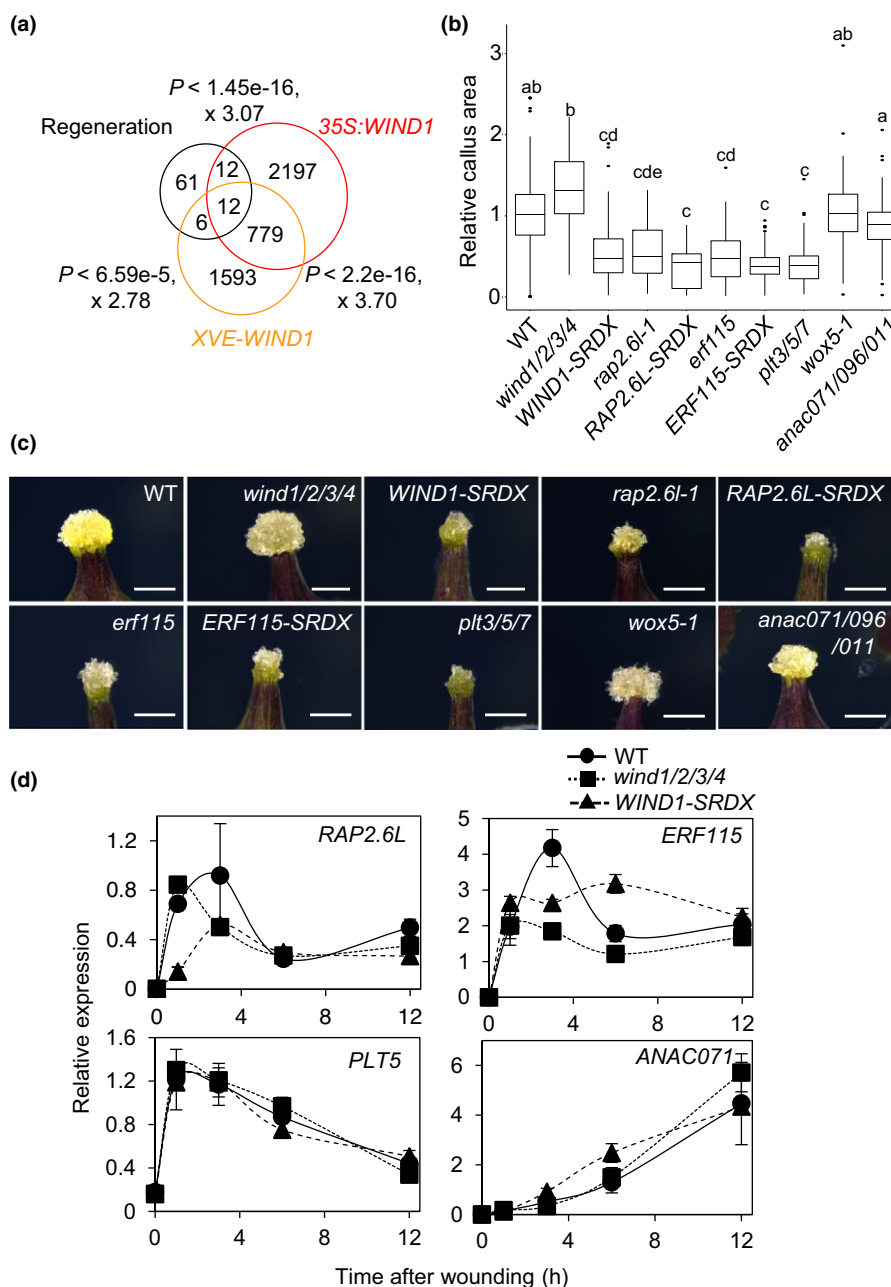
Fig. 2 WIND transcription factor-induced RAP2.6L and ERF115 promote callus formation at wound sites. (a) Venn diagram showing the overlap between WIND1-induced genes in *XVE-WIND1* seedlings, WIND1-induced genes in *35S:WIND1* callus (Iwase *et al*., 2011a) and genes implicated in reprogramming in Arabidopsis (Ikeuchi *et al*., 2019). The significance of overlap between a pair of gene sets is evaluated by Fisher's exact test, and *P*-values and odds ratio are shown. (b) Quantitative analysis of wound-induced callus formation in wild-type (WT), *wind1/2/3/4*, Pro$_{WIND1}$:WIND1-SRDX (WIND1-SRDX), *rap2.6l-1*, Pro$_{RAP2.6L}$:RAP2.6L-SRDX (RAP2.6L-SRDX), *erf115*, Pro$_{ERF115}$:ERF115-SRDX (ERF115-SRDX), *plt3/5/7*, *wox5-1* and *anac071/096/011*. Leaf explants were cultured on phytohormone-free Murashige & Skoog (MS) medium and callus phenotypes were scored at 8 d after wounding. Box plots represent the distribution of projected callus area (*n* = 33 to 352 per genotype); horizontal line shows median, the lower and upper bounds of each box plot denote the first and third quartiles, and whiskers above and below the box plot indicate 1.5 times the interquartile range. Outliers are shown as dots. Letters indicate statistical significance determined by ANOVA and Tukey's multi-comparison test (*P* < 0.05). (c) Representative images of wound-induced callus generated in WT, *wind1/2/3/4*, Pro$_{WIND1}$:WIND1-SRDX (WIND1-SRDX), *rap2.6l-1*, Pro$_{RAP2.6L}$:RAP2.6L-SRDX (RAP2.6L-SRDX), *erf115*, Pro$_{ERF115}$:ERF115-SRDX (ERF115-SRDX), *plt3/5/7*, *wox5-1* and *anac071/096/011* leaf explants. Photographs are taken at 8 d after cutting leaf petioles. Bars, 1 mm. (d) Reverse transcription quantitative polymerase chain reaction (RT-qPCR) analysis of *RAP2.6L*, *ERF115*, *PLT5* and *ANAC071* expression after wounding. First and second leaves of 14-d-old WT *wind1/2/3/4* and *WIND1-SRDX* seedlings were cut and leaf explants were cultured on phytohormone-free MS medium. Expression levels are normalized against those of the *PP2AA3* gene. Data are mean ± SE (*n* = 3, biological replicates).

whether WIND1 can induce their expression in a transient trans-activation assay. We constructed the luciferase reporter plasmids to drive the expression of luciferase proteins by 3 kb upstream sequence of the candidate genes and co-bombarded these plasmids with the *WIND1* effector plasmids into Arabidopsis suspension cells. *WIND1* overexpression significantly increased the luciferase activity in five out of the six genes tested, when compared to the control plasmids (Fig. 1d). This indicates that WIND1 can activate the promoter in five of the tested wound-induced genes either directly or indirectly.

WIND1 induces multiple reprogramming regulators to promote callus formation

WIND1 promotes diverse modes of regeneration including callus formation, shoot and root regeneration, and somatic embryogenesis (Iwase et al., 2011a, 2013, 2015; Ikeuchi *et al.*, 2013). WIND1 induces *ESR1* expression to promote callus formation and shoot regeneration (Iwase *et al.*, 2017) but it could also affect expression of other reprogramming regulators. Indeed, our Venn diagram analysis showed that 30 out of 91 reprogramming regulators in Arabidopsis (Ikeuchi *et al.*, 2019) were highly upregulated in *XVE-WIND1* seedlings and/or *35S:WIND1* callus (Iwase *et al.*, 2011a) (Fig. 2a; Table 1). As expected, this list of WIND1-induced reprogramming regulators included *ESR1*, and we found many other key transcriptional regulators, such as *LBD18*, *OBF BINDING PROTEIN 4* (*OBP4*), *ESR2*, *RAP2.6L*, *ERF115*, *WUSCHEL* (*WUS*), *PLT5*, *WUSCHEL-RELATED HOMEOBOX 5* (*WOX5*), *LEAFY COTYLDEON 2* (*LEC2*) and *Arabidopsis NAC DOMAIN CONTAINING PROTEIN 71* (*ANAC071*), which were expressed within 24 h after *WIND1* induction (Table 1). We have previously shown that WIND1 enhances the cytokinin response near wound sites (Iwase *et al.*, 2011a) and consistently, cytokinin biosynthesis genes, *LONELY GUY 1* (*LOG1*) and *LOG4,* were induced by *WIND1* overexpression within 6 h (Table 1). WIND1 may, in addition, regulate auxin homeostasis during regeneration since an auxin biosynthesis gene, *YUCCA4* (*YUC4*), and the transport gene, *PIN-FORMED 1* (*PIN1*), were also activated by 6 h after *WIND1* induction. Finally, consistent with the upregulation of *ERF115* and *ANAC071* by WIND1, their downstream target genes such as the wound-responsible small peptide *PHYTOSULFOKINE 5* (*PSK5*; Loivamäki *et al.*, 2010; Heyman *et al.*, 2013), *XYLOGLUCAN ENDOTRANSGLUCOSYLASE/HYDROLASE 19* (*XTH19*) and *XTH20* (Pitaksaringkarn *et al.*, 2014), were induced within 24 h after *WIND1* induction (Table 1). These results strongly suggest that WIND1 activates a multifaceted set of reprogramming regulators to promote cell proliferation and cell wall remodeling during regeneration.

Since WIND1 is required for callus induction at wound sites (Iwase *et al.*, 2011a), we next asked whether WIND1-targetted reprogramming regulators participate in wound-induced callus formation. As previously reported (Iwase *et al.*, 2011a, 2017), WT leaf explants generated a large mass of callus cells at wound sites while the *WIND1-SRDX* plants in which WIND1 function is dominantly repressed by the WIND1-SRDX chimeric proteins

showed smaller callus at wound site (Fig. 2b,c). We also confirmed that the *wind1 wind2 wind3 wind4* quadruple mutant (hereafter referred to as *wind1/2/3/4*) was not defective in the wound-induced callus (Iwase *et al.*, 2011a). Given that this quadruple mutant line showed clear reduction in expression levels of each *WIND* genes (Fig. S2a), this suggests there are functionally redundant factors which enhance callus formation other than WIND transcription factors in wounded petiole. Strikingly, callus formation was significantly compromised in leaf explants of *rap2.6l-1/erf113*, *RAP2.6L-SRDX*, *erf115*, *ERF115-SRDX* and *plt3 plt5 plt7* triple mutant (hereafter referred to as *plt3/5/7*) loss-of-function mutants (Fig. 2b,c), clearly demonstrating the requirement of RAP2.6L, ERF115, and PLT proteins in wound-induced callus formation. By contrast, *wox5-1* and *anac071 anac096 anac011* triple mutant (hereafter referred to as *anac071/096/011*) loss-of-function mutants showed no significant difference in callus formation compared to WT (Fig. 2b,c), indicating that these transcriptional regulators are dispensable for wound-induced callus formation in Arabidopsis leaf petioles. We should note that both ERF115 and PLTs are required for callus formation in wounded hypocotyls but RAP2.6L is unessential (Ikeuchi *et al.*, 2017). This indicates that tissue specific regulatory mechanisms exist for wound-induced callus formation.

To investigate whether these WIND1-targetted genes are induced by wounding, we quantified their expression levels in wounded leaf petioles. Our RT-qPCR analysis showed that several tested genes, including *RAP2.6L*, *ERF115* and *PLT5,* were induced within 1 h in response to wounding and declined after 3 h (Fig. 2d). By contrast, the expression of *ANAC071* was induced more slowly after wounding and its transcript level continued to increase up to 12 h (Fig. 2d). We did observe clear downregulation of *RAP2.6L* and *ERF115* expression in the WIND1-SRDX and *wind1/2/3/4* plants (Fig. 2d), indicating that WIND transcription factors are required for their upregulation upon wounding. Overall, these data suggest that wound stress induces multiple WIND1 downstream genes through robust transcriptional mechanisms and loss of WIND transcription factor function is insufficient to block their wound-induced expression. Interestingly, *RAP2.6*, a close homolog of *RAP2.6L/ERF113* and *ERF115* within the ERF subfamily X, was strongly induced by wounding and suppressed in the WIND1-SRDX but neither its loss-of-function nor gain-of-function mutants displayed any defects in wound-induced callus formation (Fig. S2b, c). These data thus demonstrate that WIND transcription factors selectively utilize RAP2.6L and ERF115 among this subfamily for callus formation.

WIND transcription factors promote xylem reconnection

Strong enrichment of cell wall-related genes among WIND1-induced genes suggests that WIND1 participates in the remodeling of cell walls after wounding. The formation of vasculatures in tissues near wound sites is the post-wound process that involves dynamic deposition and modification of cell wall polysaccharides (Lipetz, 1970). Our Venn diagram analysis indeed revealed that genes upregulated in either *XVE-WIND1* or *35S:WIND1* plants

New
Phytologist

Table 1 Heat-map representation of WIND1-induced transcriptional changes for genes implicated in regeneration.

AGI	Name	Protein description	Function in regeneration	Fold change						References
				XVE:WIND1[a]					35S:WIND1[b]	
				1	3	6	12	24 (h)		
AT1G78080	WIND1	AP2/ERF	callus, shoot, root, somatic embryo	2.1	2.2	2.5	3.0	2.9	5.8	Iwase et al., (2011a), (2017); Ikeuchi et al., (2013)
AT1G36060	WIND3	AP2/ERF	callus	0.5	0.9	0.8	0.6	1.2	28.6	Iwase et al., (2011a)
AT5G65130	WIND4	AP2/ERF	callus	1.1	1.0	1.2	1.3	1.5	5.0	Iwase et al., (2011a), (2011b)
AT1G12980	ESR1	AP2/ERF	callus, shoot	1.2	0.6	2.6	0.8	1.7	344.2	Banno et al., (2001); Iwase et al., (2017)
AT1G24590	ESR2	AP2/ERF	callus, shoot	1.7	0.4	2.3	0.9	1.1	27.1	Ikeda et al., (2006)
AT5G13330	RAP2.6L	AP2/ERF	shoot, grafting	1.3	0.9	1.2	1.4	2.6	45.7	Che et al., (2006); Asahina et al., (2011)
AT5G07310	ERF115	AP2/ERF	callus, root	1.1	1.0	7.0	22.6	19.7	83.5	Heyman et al., (2016); Ikeuchi et al., (2017)
AT5G10510	PLT3	AP2/ERF	callus, shoot	0.8	0.8	1.0	0.8	1.0	8.0	Kareem et al., (2015); Ikeuchi et al., (2017)
AT5G57390	PLT5	AP2/ERF	callus, shoot, somatic embryo	1.0	0.9	1.7	1.8	3.2	17.6	Kareem et al., (2015); Ikeuchi et al., (2017)
AT5G65510	PLT7	AP2/ERF	callus, shoot	1.0	0.6	1.4	0.8	1.3	36.6	Kareem et al., (2015); Ikeuchi et al., (2017)
AT1G19850	MP	ARF	root	0.9	0.9	1.4	0.9	1.4	4.9	Efroni et al., (2016)
AT1G28300	LEC2	B3	embryogenesis	0.6	1.2	1.2	2.7	7.2	1.3	Stone et al., (2001); Braybrook et al., (2006)
AT5G60850	OBP4	DOF	callus	1.6	1.7	1.8	2.9	2.2	1.1	Ramirez-Parra et al., (2017)
AT1G62360	STM	HD	shoot	0.9	0.8	1.1	0.6	1.0	16.2	Zhang et al., (2017)
AT2G17950	WUS	HD	callus, shoot, somatic embryo	1.2	0.7	1.0	1.4	2.7	482.6	Gallois et al., (2004); Gordon et al., (2007)
AT3G11260	WOX5	HD	root, shoot	1.7	1.9	2.8	2.0	3.9	18.3	Hu et al., (2016); Kim et al.,(2018)
AT5G05770	WOX7	HD	root, shoot	0.8	0.6	1.0	1.0	1.3	7.7	Hu et al., (2016); Kim et al.,(2018)
AT2G45420	LBD18	LBD	callus	1.0	1.0	1.2	3.1	3.1	2.4	Fan et al.,(2012)
AT3G15170	CUC1	NAC	shoot	0.8	0.8	1.0	0.8	1.0	104.8	Daimon et al., (2003)
AT5G53950	CUC2	NAC	shoot	1.1	0.7	1.3	0.8	0.8	32.4	Daimon et al., (2003); Kareem et al., (2015)
AT4G17980	ANAC071	NAC	grafting	0.9	0.9	1.1	2.0	2.0	24.8	Asahina et al., (2011); Pitaksaringkarn et al.,(2014)
AT2G28305	LOG1	cyokinin biosynthesis	callus	1.3	1.5	2.1	2.5	2.1	0.1	Ikeuchi et al.,(2017)
AT3G53450	LOG4	cyokinin biosynthesis	callus	1.6	1.2	1.6	1.8	3.4	6.0	Ikeuchi et al.,(2017)
AT5G11320	YUC4	auxin biosynthesis	callus, shoot, somatic embryo	0.9	1.4	4.2	4.8	6.3	11.3	Bai et al.,(2013); Chen et al., (2016)
AT1G21430	YUC11	auxin biosynthesis	somatic embryo	1.0	1.0	1.0	1.0	1.2	4.8	Bai et al.,(2013)
AT1G73590	PIN1	auxin transporter	root, shoot, somatic embryo	1.1	1.2	2.0	2.1	1.8	2.7	Su et al.,(2009); Bustillo-Avendaño et al.,(2017)
AT5G50260	CEP1	cysteine peptidase	root	0.7	1.9	1.4	1.7	1.9	11.4	Chen et al., (2016)
AT5G65870	PSK5	peptide hormone	root	1.9	1.9	1.3	2.8	4.2	11.7	Heyman et al., (2016)
AT4G30290	XTH19	xyloglucan transglucosylase/hydorase	grafting	1.0	1.6	2.9	2.8	8.2	9.7	Pitaksaringkarn et al.,(2014)
AT5G48070	XTH20	xyloglucan transglucosylase/hydorase	grafting	1.0	2.3	2.1	4.5	5.4	1.2	Pitaksaringkarn et al.,(2014)

Legend: >18.89; >10.49; >5.83; >3.24; >1.80; >0.55; <0.55; <0.30; <0.17; <0.09; <0.05

Among genes implicated in reprogramming in Arabidopsis (Ikeuchi et al., 2019), those induced by WIND1 are listed.
[a]Gene expression in XVE-WIND1 seedlings at 1, 3, 6, 12 and 24 h after 17-β-estradiol (ED) treatment. Fold change, relative to dimethyl sulfoxide (DMSO)-treated XVE-WIND1 seedlings, is shown.
[b]Gene expression in 35S:WIND1 callus. Fold change, relative to wild-type (WT) seedlings, is shown.

significantly overlapped with those induced during vascular formation in the VISUAL system (Fig. 3a; Tables 2, S3). Importantly, WIND1 induces several key transcriptional regulators implicated in vascular formation including VND6, VND7 and LBD30 (Kubo et al., 2005; Soyano et al., 2008) (Table 2), strongly suggesting that WIND1 promotes vascular development. Consistent with this transcriptional activation, we found that overexpression of WIND1 induced ectopic formation of tracheary elements in both XVE-WIND1 and 35S:WIND1 plants (Figs 3b, S3a). Importantly, tracheary elements can be formed from differentiated cells such as leaf mesophyll cells and root hair cells (Figs 3b, S3a), confirming the strong reprogramming capability of WIND1.

Our time-course RT-qPCR analysis further showed that WIND1 expression itself is strongly induced within 1 h after seedlings were transferred to the VISUAL condition (Fig. S3b), implying that WIND1 functions at an early step during vascular formation in this experimental setup. We, therefore, compared the tracheary element formation between WT, WIND1-SRDX and wind1/2/3/4 plants under the VISUAL condition and observed significant reduction in leaf mesophyll cells of both WIND1-SRDX and wind1/2/3/4 plants (Figs 3c,d, S3c). We also found that the expression of several key genes in xylem formation, for example IRX3, XCP1, VND7 and LBD15, was compromised in WIND1-SRDX plants (Fig. S3d), further corroborating that WIND transcription factors and functional redundant factors activate key transcriptional regulators in vascular formation. By contrast, expression of genes implicated in cambium development, that is,

TDR and AtHB8, or phloem development, that is, SEOR1, APL and SMXL5, was comparable between WT and WIND1-SRDX plants (Fig. S3d), supporting the idea that WIND1 selectively promotes xylem formation in the VISUAL system.

To examine whether WIND transcription factors contribute to vascular formation after wounding, we developed an experimental system which enabled the assessment of vascular reconnection (Fig. 3e). In this system, cut leaf petioles were forced to graft within a silicon tube. Using this assay, c. 80% of WT, wind1 single knockout and wind1/2/3/4 quadruple mutant leaf petioles were physically reconnected, while only 62% of WIND1-SRDX petioles managed to reconnect (Fig. 3f). We also observed xylem reconnection at the graft junction by examining the transport of a florescent dye from roots to the grafted leaves (Fig. 3e). We found that 39% of WT petioles transported the dye into grafted leaves. Phloroglucinol staining confirmed xylem reconnection is achieved by bridge of tracheary elements between stock and leaf petiole scission (Fig. S3e). Importantly, only 24% of WIND1-SRDX petioles succeeded. Moreover, wind1/2/3/4 and wind1 mutant significantly reduced vascular reconnection rate to 5% and 19%, respectively (Fig. 3f), clearly indicating an involvement of WIND1 and other WIND homologs in xylem reconnection in wound-induced petiole callus (Fig. 3f). We also found that wound-induced expression of VND6, VND7 and LBD30 were significantly reduced in WIND1-SRDX plants but not in wind1/2/3/4, suggesting upregulation of these key transcription factors soon after wounding by functionary redundant factors other than WIND transcription factors.
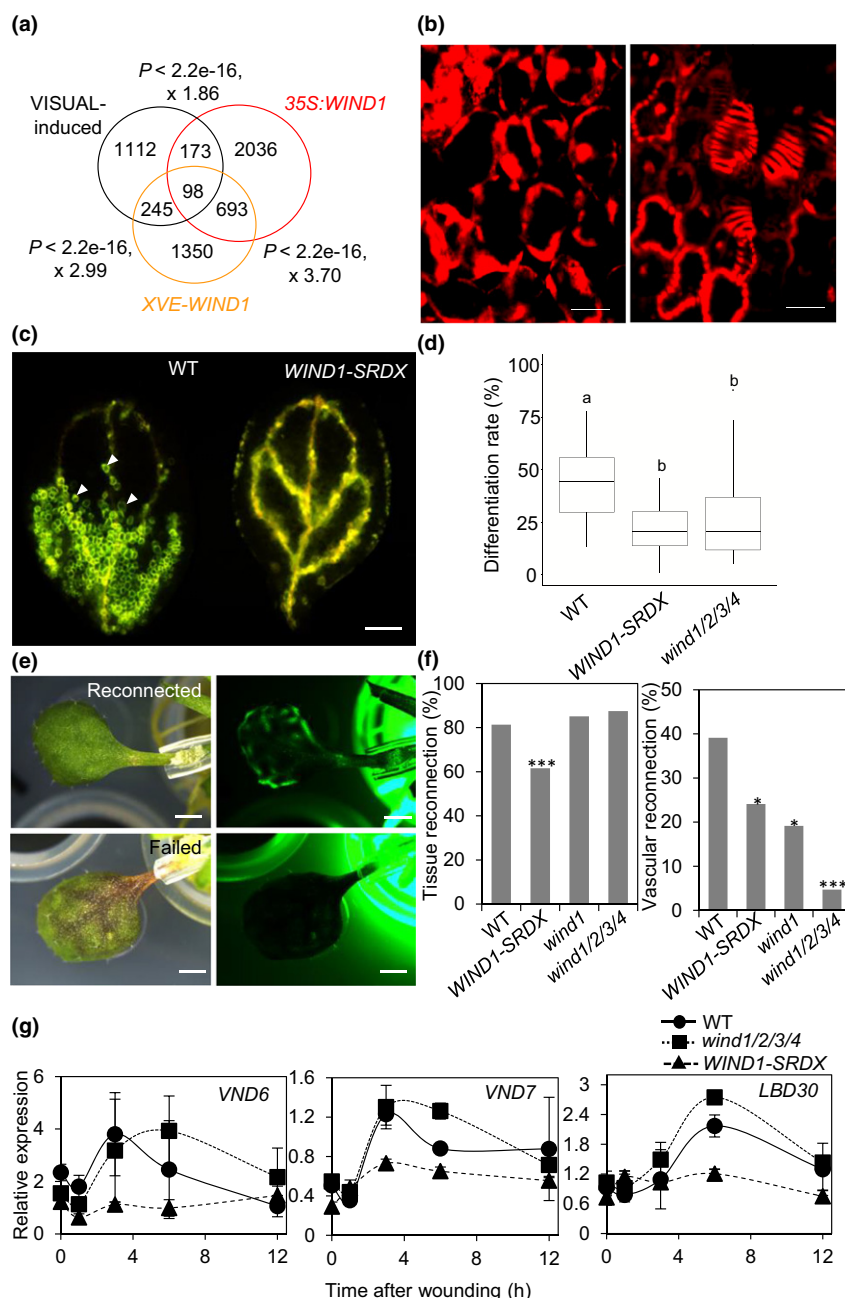
Fig. 3 WIND transcription factors induce key regulators of xylem differentiation and promotes leaf petiole grafting. (a) Venn diagram showing the overlap between WIND1-induced genes in *XVE-WIND1* seedlings, WIND1-induced genes in *35S:WIND1* callus (Iwase *et al*., 2011a) and genes induced during vascular development under the Vascular Cell Induction Culture System Using Arabidopsis Leaves (VISUAL) condition (Kondo *et al*., 2015, 2016). The significance of overlap between a pair of gene sets is evaluated by Fisher's exact test, and *P*-values and odds ratio are shown. (b) Confocal optical sections of propidium iodide (PI)-labeled mesophyll cells in *XVE-WIND1* cotyledons. *XVE-WIND1* seedlings were germinated in the presence of dimethyl sulfoxide (DMSO) or 10 μM 17β-estradiol (ED) and tracheary element formation was visualized by PI staining in 7-d-old seedlings. Bars, 50 μm. (c) Fluorescent images of wild-type (WT) and *WIND1-SRDX* cotyledon cells cultured under the VISUAL condition. Tracheary element formation visualized by BF-170 staining were marked by arrowheads. Bars, 500 μm. (d) Quantitative analysis of xylem differentiation in WT, *WIND1-SRDX*, *wind1/2/3/4* cotyledon cells cultured under the VISUAL condition. Differentiation rate is shown as relative fluorescence intensity of BF-170 normalized by leaf area. Box plots represent the distribution of projected callus area (*n* = 66 for WT, 63 for *WIND1-SRDX* and 75 for *wind1/2/3/4*). Letters indicate statistical significance determined by ANOVA and Tukey's multi-comparison test (*P* < 0.05). (e) Experimental setup for the petiole grafting assay. Incised petioles were grafted in a silicon tube and tissue reconnection was examined after 12 d. Vascular reconnection was assessed by successful transmission of a fluorescent dye CFDA into grafted leaves. Bars, 1 mm. (f) Quantitative analysis of tissue reconnection (left) and vascular reconnection (right) in WT and *WIND1-SRDX* seedlings. Statistical significance is determined by a proportion test (*n* = 161 for WT, 112 for *WIND1-SRDX*, 47 for *wind1* and 64 for *wind1/2/3/4*; *, *P* < 0.05; ***, *P* < 0.001). (g) Reverse transcription quantitative polymerase chain reaction (RT-qPCR) analysis of *VND6*, *VND7* and *LBD30* expression after wounding. First and second leaves of 14-d-old WT, *WIND1-SRDX* and *wind1/2/3/4* seedlings were cut and leaf explants were cultured on phytohormone-free Murashige & Skoog (MS) medium. Expression levels are normalized against those of the *PP2AA3* gene. Data are mean ± SE (*n* = 3, biological replicates).

Table 2 Heat-map representation of WIND1-induced transcriptional changes for genes implicated in vascular development.

AGI	Name	Protein description	Fold change					
			XVE:WIND1[a]					35S:WIND[b]
			1	3	6	12	24 (h)	
AT1G12890		AP2_ERF	1.49	0.68	1.06	0.78	1.23	56.96
AT4G28140		AP2_ERF	4.76	54.31	42.9	30.3	63.79	14.68
AT5G07310	ERF115	AP2_ERF	1.08	1	7.01	22.57	19.71	83.53
AT5G10510	PLT3	AP2_ERF	0.78	0.79	1.02	0.78	0.96	7.98
AT1G19850	MP	ARF	0.94	0.85	1.35	0.92	1.44	4.88
AT2G40470	LBD15	AS2	0.71	0.78	0.9	1.37	2.56	4.65
AT2G45420	LBD18	AS2	1	1.02	1.17	3.11	3.09	2.44
AT4G00220	LBD30	AS2	1.41	1.13	1.22	2.7	5.55	7.87
AT4G00200	AHL7	AT-hook	0.98	0.78	1.17	0.99	0.84	2.81
AT4G12080	AHL1	AT-hook	1.05	1.11	0.88	1.39	1.21	2.6
AT4G35390	AHL25	AT-hook	1.33	2.78	4.46	8.1	8.99	3.76
AT1G15580	IAA5	AUX_IAA	1	1.13	0.63	1.14	2.45	0.31
AT4G28640	IAA11	AUX_IAA	1.03	1.29	1.25	1.58	2.46	1.71
AT4G21550	HSI2-L2	B3	0.75	0.92	0.62	0.9	1.07	2.93
AT2G41130	bHLH106	bHLH	1	1.72	2.02	3.36	4.45	4.24
AT2G43060	IBH1	bHLH	1.24	1.15	0.95	1.33	1.3	2.48
AT4G28790	bHLH023	bHLH	0.77	0.81	0.44	0.42	0.59	27.52
AT1G77920	TGA7	bZIP	1.05	1.07	0.81	0.89	0.99	3.78
AT3G60580		C2H2ZnF	0.86	1.94	2.76	3.96	3.66	1.56
AT4G16610		C2H2ZnF	0.55	0.8	0.9	1.15	1.22	4.25
AT5G03510		C2H2ZnF	0.74	0.76	0.98	1.76	2.99	2.5
AT5G60470	AtIDD13	C2H2ZnF	1.09	0.76	1.37	1.57	3.05	17.21
AT1G66810	AtC3H14	C3HZnF	1.06	1.02	1.3	2.35	1.98	1.68
AT2G19810	OZF1	C3HZnF	1.37	0.98	0.86	0.69	0.54	3.2
AT5G49200		C3HZnF	0.6	0.67	1.37	1.3	4.23	7.2
AT4G00940	ITD1	DOF	0.83	0.54	0.7	0.47	0.52	5.22
AT4G36620	GATA19	GATA	0.72	0.96	2.12	3.46	1.53	0.52
AT4G35550	WOX13	HD	1.34	2.75	4.62	4.55	5.03	2.1
AT3G58780	SHP1	MADS	0.77	1.23	0.93	0.57	0.9	40.02
AT1G63910	AtMYB103	MYB	1.18	0.89	1.26	2.47	3.46	6.43
AT1G66230	MYB20	MYB	2.45	2.02	4.2	5.54	5.05	4.48
AT2G16720	MYB7	MYB	1.61	1.55	1.56	2.4	3.23	2.46
AT3G08500	MYB83	MYB	0.88	0.99	1.67	4.51	3.48	2.01
AT5G12870	MYB46	MYB	1.03	1.03	2.12	6.6	5.4	10.31
AT5G16600	MYB43	MYB	1.22	1.36	1.79	1.83	2.48	0.41
AT1G01010	ANAC001	NAC	1.54	3.65	5.72	7.14	8.95	6.05
AT1G02220	ANAC003	NAC	0.93	1.48	1.85	2.46	3.78	0.79
AT1G02230	ANAC004	NAC	1.27	1.73	2.31	1.78	2.13	0.89
AT1G12260	VND4	NAC	1.08	0.8	1.12	1.76	3.61	2.15
AT1G62700	VND5	NAC	1.19	0.98	1.12	2.11	2.92	2.38
AT1G71930	VND7	NAC	1.01	2.34	3.75	9.55	11.43	33.43
AT1G77450	NAC032	NAC	1.47	1.27	1.86	2.94	2.66	3.54
AT2G33480	NAC041	NAC	0.79	1.03	0.77	1.03	1.11	2.02
AT3G04060	NAC046	NAC	1.17	1.49	0.91	1.8	1.85	2.03
AT4G17980	ANAC071	NAC	0.94	0.86	1.1	1.98	2.04	24.84
AT4G36160	VND2	NAC	1.56	2.77	5.25	7.84	12.21	36.38
AT5G14000	ANAC084	NAC	0.95	0.92	0.81	1.02	1.1	5.05
AT5G46590	ANAC096	NAC	1.54	0.86	1.14	1.18	0.96	5.17
AT5G56620	ANAC099	NAC	1.51	0.97	0.9	1.29	0.87	5.1
AT5G62380	VND6	NAC	1.01	1.09	2.44	4.16	2.75	2.6
AT2G30395	OFP17	OFP	0.74	0.88	1.11	2.57	1.82	2.73
AT5G22240	OFP10	OFP	1.04	1.29	1.2	1.42	3.12	3.57
AT3G27010	TCP20	TCP	0.86	0.92	0.93	0.99	1.16	2.96
AT1G28520	VOZ1	VOZ	1.18	0.97	1.1	0.98	0.99	2.02
AT1G69810	WRKY36	WRKY	0.7	0.86	0.59	0.98	0.77	2.29
AT2G25000	WRKY60	WRKY	0.6	0.78	0.47	0.64	0.78	2.85
AT2G47260	WRKY23	WRKY	1.01	1.34	1.73	1.85	1.6	5.08
AT3G01970	WRKY45	WRKY	1.01	2.31	1.06	1.34	1.73	12.37
AT4G30935	WRKY32	WRKY	0.97	1.2	1.36	1.54	1.69	2.45
AT5G46350	WRKY8	WRKY	1.19	1.53	1.32	2.06	1.86	7.65
AT5G64810	WRKY51	WRKY	2.17	1.51	0.98	1.11	1.09	2.7

Legend:
>18.89
>10.49
>5.83
>3.24
>1.80
>0.55
<0.55
<0.30
<0.17
<0.09
<0.05

Among transcriptional regulators induced under the Vascular Cell Induction Culture System Using Arabidopsis Leaves (VISUAL) condition (Kondo et al., 2015, 2016), those induced by WIND1 are listed.
[a]Gene expression in XVE-WIND1 seedlings at 1, 3, 6, 12 and 24 h after 17-β-estradiol (ED) treatment. Fold change, relative to dimethyl sulfoxide (DMSO)-treated XVE-WIND1 seedlings, is shown.
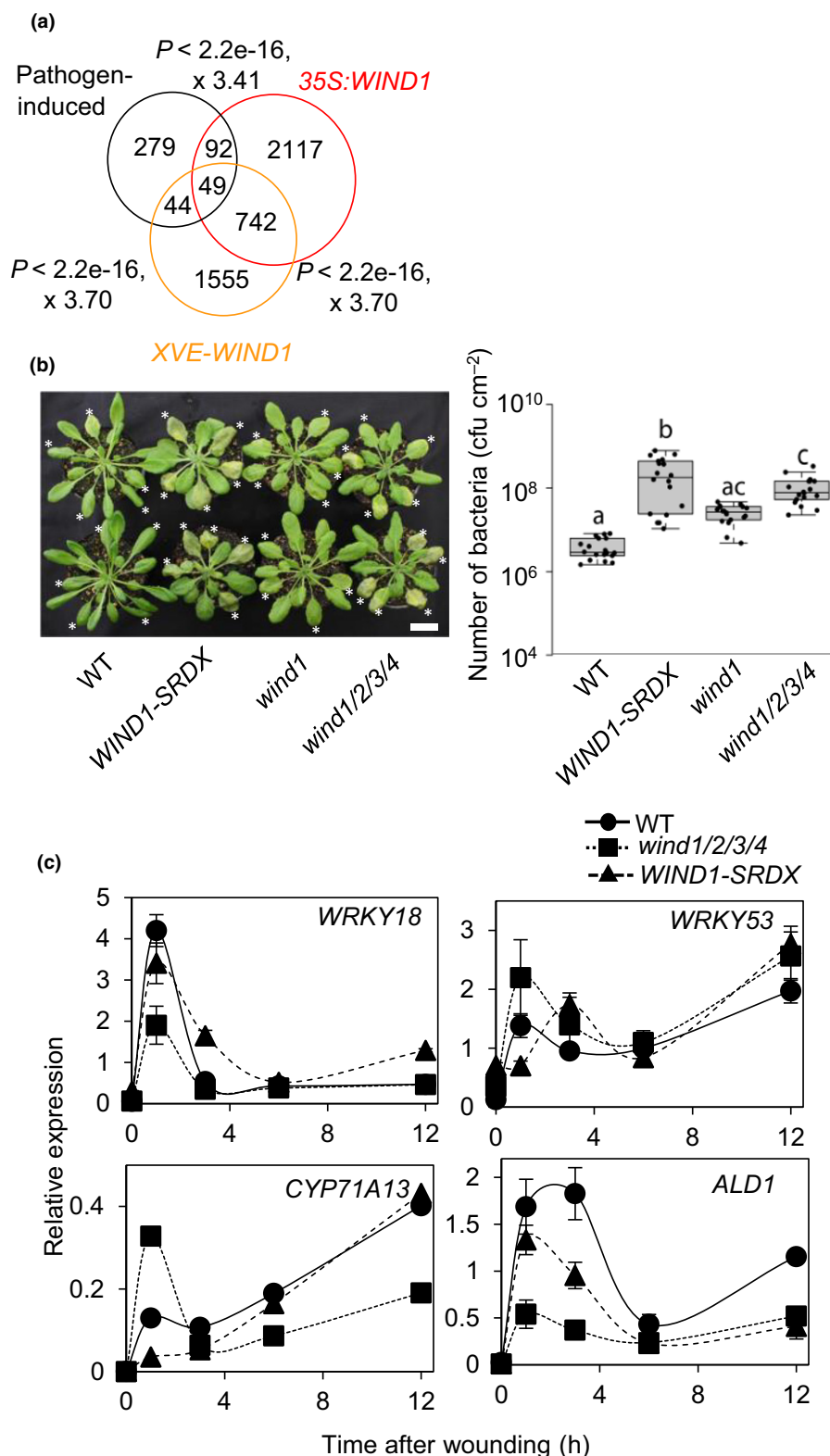[b]Gene expression in 35S:WIND1 callus. Fold change, relative to wild-type (WT) seedlings, is shown.

WIND1 induces defense response regulators to convey resistance against *Pseudomonas syringae* DC3000

Since defense response genes are enriched in WIND-induced genes (Fig. 1), we sought to explore whether WIND1 also plays a role in the resistance against pathogen infection. Defense-related genes were activated in *XVE-WIND1* or *35S:WIND1* plants (Fig. 4a; Tables 3, S4), which were significantly overlapped with those induced in response to the pathogen infection (Sato *et al.*, 2007). Importantly, *WIND1* itself was induced by pathogens

Fig. 4 WIND transcription factors induce a set of defense response regulators and promotes resistance against *Pseudomonas syringae* pv. tomato (*Pst*) DC3000. (a) Venn diagram showing the overlap between WIND1-induced genes in *XVE-WIND1* seedlings, WIND1-induced genes in *35S:WIND1* callus (Iwase *et al.*, 2011a) and genes induced in response to pathogen infection (Sato *et al.*, 2007). The significance of overlap between a pair of gene sets is evaluated by Fisher's exact test, and *P*-values and odds ratio are shown. (b) *WIND1-SRDX* and *wind1/2/3/4* are susceptible to *Pst* DC3000 infection. Bacterial growth was assessed by colony counting after 3 d of inoculation. Leaf discs were taken from three leaves per plant, with six plants per genotype per independent trial. Left, representative figures from infiltrated plants at 3 d post-inoculum. White asterisks represent *Pst* DC3000-infiltrated leaves. Right, box plots represent the colony-forming units (CFU) per cm^2 which were determined at 3 d post-inoculum; horizontal line shows median, the lower and upper bounds of each box plot denote the first and third quartiles, and whiskers above and below the box plot indicate 1.5 times the interquartile range. Individual data points are shown with mean $\pm$ SD, $n = 18$ plants from three separate trials. Letters indicate statistical significance determined by ANOVA and Tukey's multi-comparison test ($P < 0.1$). Bar, 2 cm. (c) Reverse transcription quantitative polymerase chain reaction (RT-qPCR) analysis of *WRKY18*, *WRKY53*, *CYP71A13* and *ALD1* expression after wounding. First and second leaves of 14-d-old wild-type (WT), *wind1/2/3/4* and *WIND1-SRDX* seedlings were cut and leaf explants were cultured on phytohormone-free Murashige & Skoog (MS) medium. Expression levels are normalized against those of the *PP2AA3* gene. Data are mean $\pm$ SE. ($n = 3$, biological replicates).

Table 3 Heat-map representation of WIND1-induced transcriptional changes for genes implicated in pathogen response.

AGI	Name	Protein description	Fold change					
			XVE:WIND1[a]					*35S:WIND1*[b]
			1	3	6	12	24 (h)	
AT1G43160	RAP2.6	AP2_ERF	1.59	1.12	1.49	4.67	4.3	7.85
AT1G68840	RAV2	AP2_ERF	2.08	0.76	1.28	0.67	0.43	0.69
AT1G78080	WIND1	AP2_ERF	2.05	2.15	2.47	3.01	2.9	5.75
AT3G11020	DREB2B	AP2_ERF	0.98	1.14	1.12	1.2	1.82	24.9
AT3G15210	ERF4	AP2_ERF	2.62	2.89	2.22	3.05	2.23	2.76
AT3G16770	EBP	AP2_ERF	0.9	1.16	0.61	0.72	0.92	2.67
AT4G17500	ERF-1	AP2_ERF	2.27	1.02	2.01	2.24	0.85	3.47
AT4G25480	DREB1A	AP2_ERF	2.41	1.36	0.38	0.77	0.67	2.07
AT4G36900	RAP2.10	AP2_ERF	2.41	3.28	4.18	4.32	8.3	4.8
AT5G47220	ERF2	AP2_ERF	1.67	1.01	1.68	1.32	0.49	3.09
AT1G19850	MP	ARF	0.94	0.85	1.35	0.92	1.44	4.88
AT1G10585		bHLH	1.83	0.51	1.07	1.31	0.43	35.11
AT1G27730	STZ	C2H2ZnF	1.58	1.18	3.23	5.08	2.68	9.83
AT5G04340	ZAT6	C2H2ZnF	2.65	1.72	2.28	3.8	2.4	2.38
AT2G25900	ATCTH	C3HZnF	2.42	0.8	1.17	0.99	0.53	0.21
AT2G40140	CZF1	C3HZnF	1.63	1.71	2.89	2.56	2.37	7.32
AT2G28510	AtDof2.1	DOF	0.95	0.64	0.85	0.84	1.25	7.5
AT5G60850	OBP4	DOF	1.63	1.73	1.82	2.88	2.17	1.09
AT2G46680	HB-7	HD	1.2	1.21	0.92	1.33	1.69	8.73
AT4G36990	HSF4	HSF	1.45	0.98	0.83	1.18	1.45	2.79
AT1G56650	PAP1	MYB	0.97	0.49	1.27	3.02	0.96	0.68
AT1G71030	MYBL2	MYB	2.86	1.57	1.5	2.41	0.86	0.27
AT3G06490	MYB108	MYB	1.35	0.79	2.32	1.77	1.5	4.17
AT4G27410	RD26	NAC	2.67	1.35	3.39	6.17	3.83	4.5
AT1G80590	WRKY66	WRKY	0.86	2.09	2.45	2.2	0.84	2.04
AT1G80840	WRKY40	WRKY	1.5	1.08	2.44	1.82	1.75	3.89
AT2G30250	WRKY25	WRKY	1.33	1.17	1.22	1.01	1.11	4.18
AT4G01250	WRKY22	WRKY	1.69	1.27	2.25	1.09	1.07	3.89
AT4G23810	WRKY53	WRKY	0.6	0.77	1.11	0.57	0.78	6.41
AT4G31800	WRKY18	WRKY	2.32	2.42	3.98	3.57	4.12	16.56

>18.89
>10.49
>5.83
>3.24
>1.80
>0.55
<0.55
<0.30
<0.17
<0.09
<0.05

Among transcriptional regulators induced in response to pathogen infection (Sato *et al.*, 2017), those induced by WIND1 are listed.
[a]Gene expression in *XVE-WIND1* seedlings at 1, 3, 6, 12 and 24 h after 17-β-estradiol (ED) treatment. Fold change, relative to dimethyl sulfoxide (DMSO)-treated *XVE-WIND1* seedlings, is shown.
[b]Gene expression in 35S:WIND1 callus. Fold change, relative to wild-type (WT) seedlings, is shown.

(Table 3), supporting a possible role for WIND1 in the defense response. Consistently, we found that several pathogen-responsive *WRKY* genes, including *WRKY18* and *WRKY53* (Pandey *et al.*, 2010; Abeysinghe *et al.*, 2019), were induced by WIND1 (Table 3). To test whether WIND1 is involved in the immune responses, we challenged WT, *WIND1-SRDX, wind1/2/3/4*, and *wind1* plants with a virulent bacterial pathogen *Pst* DC3000. *WIND1-SRDX* and *wind1/2/3/4* plants consistently were more susceptible to the *Pst* DC3000 infection (Figs 4b, S4a), demonstrating that WIND1 and other WIND transcription factors are required for the resistance against *Pst* DC3000 infection.

Time-course RT-qPCR analysis further showed that *WIND1* was also induced by the application of bacterial-derived flagellin peptide (flg22), a well-established pathogen-associated molecular pattern (PAMP) (Fig. S4b). As reported previously (Sato *et al.*, 2007), flg22 also induced the expression of *WRKY18* and

WRKY53 in WT plants but this induction was not significant in *WIND1-SRDX* plants (Fig. S4c), implying that gene expression could be regulated by factors, other than WIND transcription factors in flg22 treatment. Strikingly we observed similar upregulation manner of these *WRKY* genes after wounding (Fig. 4c), and *WRKY18* upregulation is significantly compromised in *wind1/2/3/4*, inferring that the WINDs-mediated transcriptional cascade is activated during post-wound defense signaling. Furthermore, we also found that *CYP71A13* and *ALD1* were wound-inducible and their expression during the early time point was impaired in *WIND1-SRDX* and *wind1/2/3/4* plants (Fig. 4c), suggesting that WIND1 may promotes a rapid production of camalexin and/or pipecolic acid at wound site. Since WIND1-inducible *RAP2.6* was also induced by pathogen or flg22 (Fig. S4c; Table 3), we tested whether it is required for the defense response against *Pst* DC3000 infection. We, however, did not observe clear defects in *rap2.6* or its close homolog mutants *RAP2.6L* (Fig. S4a). Overall, these

results suggest that WIND transcription factors positively affected defense responses, presumably via the regulation of downstream defense-related genes.

Discussion

In this study we demonstrated that WIND1 is sufficient to activate several transcriptional cascades to coordinately drive cellular reprogramming, xylem formation and defense responses against pathogen infection. Our further experiments by WIND loss-of-function mutants revealed WIND transcription factors orchestrate these physiological responses when plants are exposed to wounding or other stress conditions (Fig. 5).

Roles of WIND1 in wound-induced regeneration

We have previously shown that wounding rapidly increases *WIND1* expression to promote cellular reprogramming near wound sites (Iwase *et al.*, 2011a). In this study, we further corroborate WIND1 as an important driver of wound-induced transcription, with over 30% of WIND1-induced downstream genes are also wound-inducible (Fig. 1a,b). It is also striking that WIND1 can induce *c.* 30% of genes implicated in regeneration in Arabidopsis (Fig. 2; Table 1). This agrees with our observation that WIND1 promotes several regenerative events such as callus formation, shoot regeneration and somatic embryogenesis, and confirms the central roles that WIND1 plays in regeneration. In addition to ESR1 (Iwase *et al.*, 2017), we showed that RAP2.6L functions downstream of WIND transcription factors in wound-induced callus formation (Fig. 2) although we do not know at this point whether WIND1 and/or other WINDs directly

activates *RAP2.6L* expression. Similar to WIND1 and ESR1, RAP2.6L is required for both callus formation at wound sites and shoot regeneration under the tissue culture condition (Che *et al.*, 2006). These observations suggest that these two regenerative processes are somehow linked at the molecular level and further elucidation of how WIND1-ESR1/RAP2.6L pathway promotes these processes should clarify the underlying mechanisms. WIND1 also induces *RAP2.6*, a close homolog of RAP2.6L but neither knock-out nor overexpression caused any significant changes in callus formation (Fig. S2). A previous study has shown that RAP2.6 functions in protecting plants against nematode infection (Ali *et al.*, 2013). It is thus likely that the activation of RAP2.6L and RAP2.6, which are both WIND1-driven, transcriptionally coordinates regeneration and defense responses (Fig. 5). How these closely related homologs target different sets of genes to promote distinct physiological processes is an interesting question that should be investigated in future studies.

In addition to *RAP2.6L*, wounding induces *ERF115* and *PLT3*, *PLT5*, *PLT7* to promote callus formation at wound sites (Fig. 2; Table 1). This suggests that this group of AP2/ERF proteins plays a key role in decoding wounding signals to acquire a new developmental trajectory. Heyman *et al.* (2016) has shown that ERF115 is required to induce *WIND1* after bleomycin treatment, thus it appears that ERF115 and WIND1 form a positive feedback loop to enhance this transcriptional pathway. It is interesting that repression of *WIND* functions does not block wound-induced expression of *PLT5* (Fig. 2d). We predict that wound-induced transcriptional changes are regulated by robust, highly overlapping mechanisms and loss of WIND1 function can probably be compensated by activating alternative pathways to induce downstream gene expression. Although WIND1-SRDX should dominantly suppress transcriptional regulators that share the same *cis* elements within target promoter, there might be other transcriptional regulators that can utilize different *cis* elements to modulate target genes. Investigating the genome-wide, wound-induced transcriptome in WT, *WIND1-SRDX* and *wind1/2/3/4* will be useful to comprehensively elucidate the WIND-dependent and -independent transcriptional pathways.

Given that genes involved in JA response are highly represented among WIND1-induced genes (Fig. 1a), WIND1 may also promote JA-dependent regeneration. Recent studies unveiled an involvement of JA-mediated pathways in root tip regeneration after laser ablation and *de novo* root formation from leaf cuttings (Zhang *et al.*, 2019; Zhou *et al.*, 2019). Our previous time-course transcriptome analysis using Arabidopsis hypocotyls also showed that JA responses are activated after wounding although JA pathways are not required for callus formation in wounded hypocotyls (Ikeuchi *et al.*, 2017). These results thus imply the existence of context-dependent regeneration mechanisms (Ikeuchi *et al.*, 2020) and an involvement of WIND1-induced JA pathways should be tested in various regeneration contexts.

Our recent studies have uncovered that plants possess an epigenetic mechanism to suppress the expression of reprogramming regulators in somatic tissues and that cell reprogramming after wounding accompanies dynamic alterations in the histone modification status (Ikeuchi *et al.*, 2015; Rymen *et al.*, 2019). It is thus
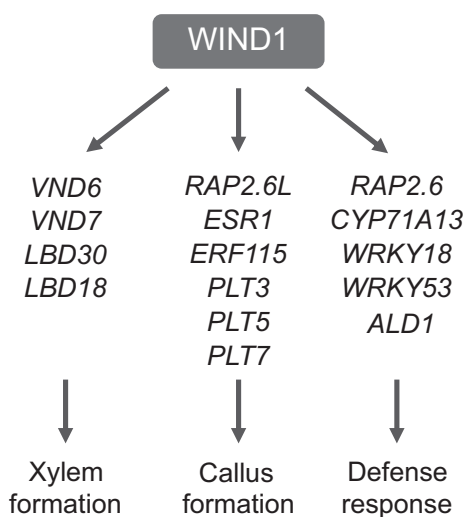
Fig. 5 A schematic model describing how WIND1 promotes multiple physiological responses. Our transcriptome-based analysis in this study reveals that WIND1 has a potential to activate reprogramming regulators such as *RAP2.6L*, *ESR1*, *ERF115*, *PLT3*, *PLT5* and *PLT7* to promote callus formation. WIND1 is also able to upregulate master regulators of xylem differentiation, including *VND6*, *VND7*, *LBD18* and *LBD30*, to promote tracheary element formation. WIND1, in addition, promotes defense response against pathogens by activating a set of key regulators such as *RAP2.6*, *CYP71A13*, *WRKY18*, *WRKY53* and *ALD1*.

interesting to note that many of WIND1 downstream target genes we identified in this study, including *RAP2.6L,* have repressive histone marks, that is, H3K27me3, before wounding and quickly gain permissive acetylation marks, that is, H3K9/14ac and H3K27ac, within a few hours after wounding (Rymen *et al.*, 2019). Future studies should thus clarify which downstream genes are directly regulated by WIND1 and WIND1 homologs and whether these transcriptional regulations involve epigenetic mechanisms. A recent study in the acoel *Hofstenia miamia* revealed that a master regulator of wound-induced regeneration is quickly expressed along wound sites and functions as a pioneering factor to open the chromatin around target loci (Gehrke *et al.*, 2019). Testing whether WIND transcription factors perform similar roles as a pioneering factor is an exciting future direction, allowing us to deepen our molecular understanding of how plants regulate wound-induced transcription.

Newly uncovered roles of WIND1 in wound-triggered responses

Alterations of cell wall composition and structure are one of the key features that accompany cell differentiation and morphogenesis in plants (Tucker *et al.*, 2018). Recent studies have begun to reveal that changes in this status can modulate various extracellular signaling pathways to modify plant growth and stress responses accordingly (De Lorenzo *et al.*, 2019). It is therefore conceivable that cells near wound sites change the cell wall status to transduce various wound-induced signaling. In support of this idea, several mutants with defects in cell wall biogenesis and/or modification show spontaneous callus formation on phytohormone free medium (Krupková & Schmülling, 2009; Ikeuchi *et al.*, 2013), suggesting that the cell wall status do influence the regenerative processes. Given that the cell wall-related genes are significantly enriched among WIND1-induced gene sets (Fig. 1b), we speculate that WIND transcription factors may also regulate regeneration by modifying the cell wall status. Consistently, we observed failure in the tissue reconnection in the petioles of *WIND1-SRDX* plants (Fig. 3e,f), demonstrating the requirement of WIND transcription factors and other functional redundant factors to reconnect two existing cell walls. Putative downstream targets of WIND1 also include XTH19 and XTH20, which are members of xyloglucan endotransglucosylase/hydrolases (Table 1). Since their loss-of-function mutants are impaired in fusing incised Arabidopsis stems (Pitaksaringkarn *et al.*, 2014), WIND1 may modulate their expression to remodel the xyloglucan structure and thus interweave closely located cell walls. Further investigation of how WIND transcription factors change the cell wall structure and composition should uncover previously unknown, cell wall-based mechanisms that underlie wound-induced regenerative processes.

Another important role of WIND1 and other homologs uncovered in this study is its involvement in wound-induced vascular reformation (Fig. 3f). This is interesting because wounding was thought to be one of the triggers for tracheary element formation (Fukuda, 1997) but underlying molecular mechanisms remained elusive. Our data show that wounding stress induces expression of *VND6, VND7* and *LBD30* and their expression level is retarded in

WIND1-SRDX line but not in *wind1/2/3/4* (Fig. 3g), suggesting that the wounding-triggered VND/LBD pathway promotes xylem formation via functional redundant factors of WIND transcription factors. Our data based on the VISUAL system implies that this WIND-related regulation specifically works on xylem cell formation, rather than cambium stem cell and phloem cell formation (Fig. S3). Intriguingly, tracheary element formation does not occur in every cell in *35S:WIND1* or *XVE:WIND1* plants, and in fact, we often observe both callus cells and cells committing to the tracheary element formation in a mosaic fashion (Fig. S3a; Ikeuchi *et al.*, 2015). How *WIND* genes overexpression promotes different cell fate is a key question that should be addressed in future studies. Of note, we observed that even detached leaf explants that failed vascular reconnection often showed tight tissue reconnection in our petiole grafting system. Moreover, the *wind1/2/3/4* mutant displayed strong defects in vascular reconnection but not in tissue reconnection (Fig. 3). We thus believe that tissue connectivity is also regulated by other factors such as callus qualities (e.g. size of the callus, type of callus cells, composition of cell walls) and not necessarily by vascular connectivity. In support of this idea, the WIND1-SRDX plants showed smaller callus at wound petiole (Fig. 2b,c) so this might be one of the reasons why they showed reduced tissue reconnection.

We also demonstrated that WIND1 induces a large set of pathogen-responsive genes and WIND transcription factors modulate resistance against *Pst* DC3000 infection (Tables 3, S4; Figs 4a, b, S4a). Although we could not test whether the WIND transcription factors-mediated pathways participate in the wound-induced defense responses, we anticipate this is very likely, given that wounding strongly induces expression of *WIND* genes and their downstream pathogen response regulators (Fig. 4c). Of note that there are clear differences of gene expression patterns after flg22 treatment or wounding, for instance *CYP71A13, ALD1* and *RAP2.6* (Figs 4c, S2b, S4c). This indicates that the degrees of WINDs involvement to trigger the immunity-related gene expression differ between flg22 treatment and wounding.

Altogether, this study establishes WIND1 as a positive regulator of wound-induced responses since WIND1 can regulate both cellular reprogramming and immune-related responses. Since injury involves the risk of infection by pathogens from the wounded site, it makes physiological sense to simultaneously enhance *de novo* tissue/organ regeneration and the immune response at the site of injury. For example, a mammalian transcription factor Hypoxia-inducible factor (HIF)-1 is upregulated in response to injury and is known to have a wide range of functions, including regeneration of the wound site, angiogenesis and activation of humoral immunity (Hellwig-Burgel *et al.*, 2005). We predict having factors such as WINDs (for plants) or HIFs (for mammalian) that can quickly direct multiple pathways was advantageous for the survival of organisms in evolution. One molecular mechanism of how WIND1 induces a specific, yet diverse, set of genes in a given context might be that WIND1 acts in multi-protein complexes. This could, for instance, be with other transcriptional regulators and coordinately determine the target specificity. It is also interesting that *WIND1* can be induced in conditions other than wounding, such as incubation

under the VISUAL and flg22 treatment (Figs S3b, S4b). Further elucidation of its activation mechanisms, including whether WIND transcription factors regulate downstream key factors directly or indirectly, and how much expression levels of WIND genes/proteins are spatiotemporally required for the downstream phenomena, should help uncover how plants transduce multiple stress signals to regeneration and defense responses through the WINDs-mediated pathways.

Acknowledgements

Author contributions

AI and KSugimoto conceived the research and designed the experiments. AI performed plasmid construction, transient expression assay and microscopy analyses. YK, AI and HF performed VISUAL assay. AL and KShirasu performed pathogen infection assay. AI and AT performed callus formation assay. MI and AI established and performed grafting experiments. NM and AI performed gene expression analyses. KM and MA provided unpublished materials. AI and KSugimoto wrote the manuscript with input from all coauthors.

ORCID

Masashi Asahina https://orcid.org/0000-0002-1828-0966
Hiroo Fukuda https://orcid.org/0000-0002-7824-9266
Momoko Ikeuchi https://orcid.org/0000-0001-9474-5131
Akira Iwase https://orcid.org/0000-0003-3294-7939
Yuki Kondo https://orcid.org/0000-0002-7937-1722
Anuphon Laohavisit https://orcid.org/0000-0002-7707-8928
Nobutaka Mitsuda https://orcid.org/0000-0001-5689-3678
Ken Shirasu https://orcid.org/0000-0002-0349-3870
Keiko Sugimoto https://orcid.org/0000-0002-9209-8230

Data availability

The transcriptome data in this study are openly available in NCBI Gene Expression Omnibus at https://www.ncbi.nlm.nih.gov/geo/query/acc.cgi?acc=GSE167174, reference no. GSE167174.

References

Abeysinghe JK, Lam KM, Ng DWK. 2019. Differential regulation and interaction of homoeologous WRKY18 and WRKY40 in *Arabidopsis* allotetraploids and biotic stress responses. *The Plant Journal* **97**: 352–367.

Ahuja I, Kissen R, Bones AM. 2012. Phytoalexins in defense against pathogens. *Trends in Plant Science* **17**: 73–90.

Ali MA, Abbas A, Kreil DP, Bohlmann H. 2013. Overexpression of the transcription factor RAP2.6 leads to enhanced callose deposition in syncytia and enhanced resistance against the beet cyst nematode *Heterodera schachtii* in *Arabidopsis* roots. *BMC Plant Biology* **13**: 47.

Amaratunga D, Cabrera J. 2001. Analysis of data from viral DNA microchips. *Journal of the American Statistical Association* **96**: 1161–1171.

Asahina M, Azuma K, Pitaksaringkarn W, Yamazaki T, Mitsuda N, Ohme-Takagi M, Yamaguchi S, Kamiya Y, Okada K, Nishimura T et al. 2011. Spatially selective hormonal control of RAP2.6L and ANAC071 transcription factors involved in tissue reunion in *Arabidopsis*. *Proceedings of the National Academy of Sciences, USA* **108**: 16128–16132.

Bai B, Su YH, Yuan J, Zhang XS. 2013. Induction of somatic embryos in *Arabidopsis* requires local YUCCA expression mediated by the down-regulation of ethylene biosynthesis. *Molecular Plant* **6**: 1247–1260.

Banno H, Ikeda Y, Niu Q, Chua N. 2001. Overexpression of *Arabidopsis ESR1* induces initiation of shoot regeneration. *The Plant Cell* **13**: 2609–2618.

Birnbaum KD, Alvarado AS. 2008. Slicing across kingdoms: regeneration in plants and animals. *Cell* **132**: 697–710.

Bloch R. 1941. Wound healing in higher plants. *Botanical Review* **7**: 110–146.

Braybrook SA, Stone SL, Park S, Bui AQ, Le BH, Fischer RL, Goldberg RB, Harada JJ. 2006. Genes directly regulated by LEAFY COTYLEDON2 provide insight into the control of embryo maturation and somatic embryogenesis. *Proceedings of the National Academy of Sciences, USA* **103**: 3468–3473.

Bustillo-Avendaño E, Ibáñez S, Sanz O, Barross JAS, Gude I, Perianez-Rodriguez J, Micol JL, del Pozo JC, Moreno-Risueno MA, Perez-Perez JM. 2017. Regulation of hormonal control, cell reprogramming and patterning during de novo root organogenesis. *Plant Physiology* **176**: 1709–1727.

Che P, Lall S, Nettleton D, Howell S. 2006. Gene expression programs during shoot, root, and callus development in *Arabidopsis* tissue culture. *Plant Physiology* **141**: 620–637.

Chen X, Cheng J, Chen L, Zhang G, Huang H, Zhang Y, Xu L. 2016. Auxin-independent *NAC* pathway acts in response to explant-specific wounding and promotes root tip emergence during de novo root organogenesis in *Arabidopsis*. *Plant Physiology* **170**: 2136–2145.

Cheong YH, Chang H-S, Gupta R, Wang X, Zhu T, Luan S. 2002. Transcriptional profiling reveals novel interactions between wounding, pathogen, abiotic stress, and hormonal responses in *Arabidopsis*. *Plant Physiology* **129**: 661–677.

Clough SJ, Bent AF. 1998. Floral dip: a simplified method for *Agrobacterium*-mediated transformation of *Arabidopsis thaliana*. *The Plant Journal* **16**: 735–743.

Cui H, Tsuda K, Parker JE. 2015. Effector-triggered immunity: from pathogen perception to robust defense. *Annual Review of Plant Biology* **66**: 487–511.

Daimon Y, Takabe K, Tasaka M. 2003. The *CUP-SHAPED COTYLEDON* genes promote adventitious shoot formation on calli. *Plant and Cell Physiology* **44**: 113–121.

De Lorenzo G, Ferrari S, Giovannoni M, Mattei B, Cervone F. 2019. Cell wall traits that influence plant development, immunity, and bioconversion. *The Plant Journal* **97**: 134–147.

Delessert C, Wilson IW, Van Der Straeten D, Dennis ES, Dolferus R. 2004. Spatial and temporal analysis of the local response to wounding in *Arabidopsis* leaves. *Plant Molecular Biology* **55**: 165–181.

Efroni I, Mello A, Nawy T, Ip P-L, Rahni R, DelRose N, Powers A, Satija R, Birnbaum KD. 2016. Root regeneration triggers an embryo-like sequence guided by hormonal interactions. *Cell* **165**: 1721–1733.

Eisen MB, Spellman PT, Brown PO, Botstein D. 1998. Cluster analysis and display of genome-wide expression patterns. *Proceedings of the National Academy of Sciences, USA* **95**: 14863–14868.

Eulgem T, Somssich IE. 2007. Networks of WRKY transcription factors in defense signaling. *Current Opinion in Plant Biology* **10**: 366–371.

Fan M, Xu C, Xu K, Hu Y. 2012. Lateral organ boundaries domain transcription factors direct callus formation in *Arabidopsis* regeneration. *Cell Research* **22**: 1169–1180.

Fujimoto SY, Ohta M, Usui A, Shinshi H, Ohme-Takagi M. 2000. *Arabidopsis* ethylene-responsive element binding factors act as transcriptional activators or repressors of GCC box-mediated gene expression. *The Plant Cell* **12**: 393–404.

Fukuda H. 1997. Tracheary element differentiation. *Plant Biotechnology Reports* **8**: 17–21.

Gallois JL, Nora FR, Mizukami Y, Sablowski R. 2004. WUSCHEL induces shoot stem cell activity and developmental plasticity in the root meristem. *Genes & Development* **18**: 375–380.

Gehrke AR, Neverett E, Luo Y-J, Brandt A, Ricci L, Hulett RE, Gompers A, Ruby JG, Rokhsar DS, Reddien PW et al. 2019. Acoel genome reveals the regulatory landscape of whole-body regeneration. *Science* **363**: eaau6173.

Gordon SP, Heisler MG, Reddy GV, Ohno C, Das P, Meyerowitz EM. 2007. Pattern formation during *de novo* assembly of the *Arabidopsis* shoot meristem. *Development* **134**: 3539–3548.

Hanin M, Brini F, Ebel C, Toda Y, Takeda S, Masmoudi K. 2011. Plant dehydrins and stress tolerance. *Plant Signaling & Behavior* **6**: 1503–1509.

Hartmann M, Zeier T, Bernsdorff F, Reichel-Deland V, Kim D, Hohmann M, Scholten N, Schuck S, Bräutigam A, Hölzel T et al. 2018. Flavin monooxygenase-generated N-hydroxypipecolic acid is a critical element of plant systemic immunity. *Cell* **173**: 456–469.

He P, Chintamanani S, Chen Z, Zhu L, Kunkel BN, Alfano JR, Tang X, Zhou JM. 2004. Activation of a COI1-dependent pathway in *Arabidopsis* is by *Pseudomonas syringae* type III effectors and coronatine. *The Plant Journal* **37**: 589–602.

Hellwig-Burgel T, Stiehl DP, Wagner AE, Metzen E, Jelkmann W. 2005. Review: hypoxia-inducible factor-1 (HIF-1): a novel transcription factor in immune reactions. *Journal of Interferon and Cytokine Research* **25**: 297–310.

Heyman J, Canher B, Bisht A, Christiaens F, De Veylder L. 2018. Emerging role of the plant ERF transcription factors in coordinating wound defense responses and repair. *Journal of Cell Science* **131**: jcs.208215.

Heyman J, Cools T, Vandenbussche F, Heyndrickx Ks, Van Leene J, Vercauteren I, Vanderauwera S, Vandepoele K, De Jaeger G, Van Der Straeten D et al. 2013. ERF115 controls root quiescent center cell division and stem cell replenishment. *Science* **342**: 860–863.

Heyman J, Cools T, Canher B, Shavialenka S, Traas J, Vercauteren I, Van den Daele H, Persiau G, De Jaeger G, Sugimoto K et al. 2016. The heterodimeric transcription factor complex ERF115-PAT1 grants regeneration competence. *Nature Plants* **2**: 16165.

de Hoon MJL, Imoto S, Nolan J, Miyano S. 2004. Open source clustering software. *Bioinformatics* **20**: 1453–1454.

Hu X, Xu L. 2016. Transcription factors WOX11/12 directly activate WOX5/7 to promote root primordia initiation and organogenesis. *Plant Physiology* **172**: 2363–2373.

Ikeda Y, Banno H, Niu QW, Howell SH, Chua NH. 2006. The *ENHANCER OF SHOOT REGENERATION 2* gene in *Arabidopsis* regulates *CUP-SHAPED COTYLEDON 1* at the transcriptional level and controls cotyledon development. *Plant & Cell Physiology* **47**: 1443–1456.

Ikeuchi M, Favero DS, Sakamoto Y, Iwase A, Coleman D, Rymen B, Sugimoto K. 2019. Molecular mechanisms of plant regeneration. *Annual Review of Plant Biology* **70**: 377–406.

Ikeuchi M, Iwase A, Rymen B, Harashima H, Shibata M, Ohnuma M, Breuer C, Morao AK, de Lucas M, De Veylder L et al. 2015. PRC2 represses dedifferentiation of mature somatic cells in *Arabidopsis*. *Nature Plants* **1**: 15089.

Ikeuchi M, Iwase A, Rymen B, Lambolez A, Kojima M, Takebayashi Y, Heyman J, Watanabe S, Seo M, De Veylder L et al. 2017. Wounding triggers callus formation via dynamic hormonal and transcriptional changes. *Plant Physiology* **175**: 1158–1174.

Ikeuchi M, Ogawa Y, Iwase A, Sugimoto K. 2016. Plant regeneration: cellular origins and molecular mechanisms. *Development* **143**: 1442–1451.

Ikeuchi M, Rymen B, Sugimoto K. 2020. How do plants transduce wound signals to induce tissue repair and organ regeneration? *Current Opinion in Plant Biology* **57**: 72–77.

Ikeuchi M, Sugimoto K, Iwase A. 2013. Plant callus: mechanisms of induction and repression. *The Plant Cell* **25**: 3159–3173.

Iwase A, Harashima H, Ikeuchi M, Rymen B, Ohnuma M, Komaki S, Morohashi K, Kurata T, Nakata M, Ohme-Takagi M et al. 2017. WIND1 promotes shoot regeneration through transcriptional activation of *ENHANCER OF SHOOT REGENERATION1* in *Arabidopsis*. *The Plant Cell* **29**: 54–69.

Iwase A, Mita K, Nonaka S, Ikeuchi M, Koizuka C, Ohnuma M, Ezura H, Imamura J, Sugimoto K. 2015. WIND1-based acquisition of regeneration

competency in *Arabidopsis* and rapeseed. *Journal of Plant Research* **128**: 389–397.

Iwase A, Mita K, Favero DS, Mitsuda N, Sasaki R, Kobayshi M, Takebayashi Y, Kojima M, Kusano M, Oikawa A et al. 2018. WIND1 induces dynamic metabolomic reprogramming during regeneration in *Brassica napus*. *Developmental Biology* **442**: 40–52.

Iwase A, Mitsuda N, Koyama T, Hiratsu K, Kojima M, Arai T, Inoue Y, Seki M, Sakakibara H, Sugimoto K et al. 2011a. The AP2/ERF transcription factor WIND1 controls cell dedifferentiation in *Arabidopsis*. *Current Biology* **21**: 508–514.

Iwase A, Mitsuda N, Ikeuchi M, Ohnuma M, Koizuka C, Kawamoto K, Imamura J, Ezura H, Sugimoto K. 2013. *Arabidopsis* WIND1 induces callus formation in rapeseed, tomato, and tobacco. *Plant Signaling and Behavior* **8**: e27432.

Iwase A, Ohme-Takagi M, Sugimoto K. 2011b. WIND1: a key molecular switch for plant cell dedifferentiation. *Plant Signaling and Behavior* **6**: 1943–1945.

Kaku H, Nishizawa Y, Ishii-Minami N, Akimoto-Tomiyama C, Dohmae N, Takio K, Minami E, Shibuya N. 2006. Plant cells recognize chitin fragments for defense signaling through a plasma membrane receptor. *Proceedings of the National Academy of Sciences, USA* **103**: 11086–11091.

Kareem A, Durgaprasad K, Sugimoto K, Du Y, Pulianmackal A, Trivedi Z, Abhayadev P, Pinon V, Meyerowitz E, Scheres B et al. 2015. *PLETHORA* genes control regeneration by a two-step mechanism. *Current Biology* **25**: 1017–1030.

Kim J, Yang W, Forner J, Lohmann JU, Noh B, Noh Y. 2018. Epigenetic reprogramming by histone acetyltransferase HAG1/AtGCN5 is required for pluripotency acquisition in *Arabidopsis*. *EMBO Journal* e98726.

Kondo Y. 2018. Reconstitutive approach for investigating plant vascular development. *Journal of Plant Research* **131**: 23–29.

Kondo Y, Fujita T, Sugiyama M, Fukuda H. 2015. A novel system for xylem cell differentiation in *Arabidopsis thaliana*. *Molecular Plant* **8**: 612–621.

Kondo Y, Nurani AM, Saito C, Ichihashi Y, Saito M, Yamazaki K, Mitsuda N, Ohme-Takagi M, Fukuda H. 2016. Vascular cell induction culture system using *Arabidopsis* leaves (VISUAL) reveals the sequential differentiation of sieve element-like cells. *The Plant Cell* **28**: 1250–1262.

Krupková E, Schmülling T. 2009. Developmental consequences of the tumorous shoot development1 mutant, a novel allele of the cellulose-synthesizing *KORRIGAN1* gene. *Plant Molecular Biology* **71**: 641–655.

Kubo M, Udagawa M, Nishikubo N, Horiguchi G, Yamaguchi M, Ito J, Mimura T, Fukuda H, Demura T. 2005. Transcription switches for protoxylem and metaxylem vessel formation. *Genes & Development* **19**: 1855–1860.

Laohavisit A, Wakatake T, Ishihama N, Mulvey H, Takizawa K, Suzuki T, Shirasu K. 2020. Quinone perception in plants via leucine-rich-repeat receptor-like kinases. *Nature* **587**: 92–97.

Lipetz J. 1970. Wound-healing in higher plants. *International Review of Cytology* **27**: 1–28.

Loivamäki M, Stührwohldt N, Deeken R, Steffens B, Roitsch T, Hedrich R, Sauter M. 2010. A role for PSK signaling in wounding and microbial interactions in *Arabidopsis*. *Physiologia Plantarum* **139**: 348–357.

Marhava P, Hoermayer L, Yoshida S, Marhavý P, Benková E, Friml J. 2019. Re-activation of stem cell pathways for pattern restoration in plant wound healing. *Cell* **177**: 957–969.

Matsuoka K, Sato R, Matsukura Y, Kawajiri Y, Iino H, Nozawa N, Shibata K, Kondo Y, Satoh S, Asahina M. 2021. Wound-inducible ANAC071 and ANAC096 transcription factors promote cambial cell formation in incised *Arabidopsis* flowering stems. *Communications Biology* **4**: 369.

Matsuoka K, Yanagi R, Yumoto E, Yokota T, Yamane H, Satoh S, Asahina M. 2018. *RAP2.6L* and jasmonic acid–responsive genes are expressed upon *Arabidopsis* hypocotyl grafting but are not needed for cell proliferation related to healing. *Plant Molecular Biology* **96**: 531–542.

Mazur E, Benková E, Friml J. 2016. Vascular cambium regeneration and vessel formation in wounded inflorescence stems of *Arabidopsis*. *Scientific Reports* **6**: 33754.

Melnyk CW. 2017. Connecting the plant vasculature to friend or foe. *New Phytologist* **213**: 1611–1617.

Melnyk CW, Gabel A, Hardcastle TJ, Robinson S, Miyashima S, Grosse I, Meyerowitz EM. 2018. Transcriptome dynamics at *Arabidopsis* graft junctions reveal an intertissue recognition mechanism that activates vascular regeneration. *Proceedings of the National Academy of Sciences, USA* 115: E2447–E2456.

Melnyk CW, Schuster C, Leyser O, Meyerowitz EM. 2015. A developmental framework for graft formation and vascular reconnection in *Arabidopsis thaliana*. *Current Biology* 25: 1306–1318.

Mitsuda N, Hiratsu K, Todaka D, Nakashima K, Yamaguchi-Shinozaki K, Ohme-Takagi M. 2006. Efficient production of male and female sterile plants by expression of a chimeric repressor in *Arabidopsis* and rice. *Plant Biotechnology Journal* 4: 325–332.

Mitsuda N, Seki M, Shinozaki K, Ohme-takagi M. 2005. The NAC transcription factors NST1 and NST2 of *Arabidopsis* regulate secondary wall thickenings and are required for anther dehiscence. *The Plant Cell* 17: 2993–3006.

Miyashima S, Roszak P, Sevilem I, Toyokura K, Blob B, Heo J-o, Mellor N, Help-Rinta-Rahko H, Otero S, Smet W *et al.* 2019. Mobile PEAR transcription factors integrate positional cues to prime cambial growth. *Nature* 565: 490–494.

Murray SL, Ingle RA, Petersen LN, Denby KJ. 2007. Basal resistance against *Pseudomonas syringae* in *Arabidopsis* involves WRKY53 and a protein with homology to a nematode resistance protein. *Molecular Plant–Microbe Interactions* 20: 1431–1438.

Návarová H, Bernsdorff F, Döring AC, Zeier J. 2012. Pipecolic acid, an endogenous mediator of defense amplification and priming, is a critical regulator of inducible plant immunity. *The Plant Cell* 24: 5123–5141.

Nurani AM, Ozawa Y, Furuya T, Sakamoto Y, Ebine K, Matsunaga S, Ueda T, Fukuda H, Kondo Y. 2020. Deep imaging analysis in VISUAL reveals the role of *YABBY* genes in vascular stem cell fate determination. *Plant and Cell Physiology* 61: 255–264.

Ohta M, Matsui K, Hiratsu K, Shinshi H, Ohme-Takagi M. 2001. Repression domains of class II ERF transcriptional repressors share an essential motif for active repression. *The Plant Cell* 13: 1959–1968.

Pandey SP, Roccaro M, Schön M, Logemann E, Somssich IE. 2010. Transcriptional reprogramming regulated by WRKY18 and WRKY40 facilitates powdery mildew infection of *Arabidopsis. The Plant Journal* 64: 912–923.

Pitaksaringkarn W, Matsuoka K, Asahina M, Miura K, Sage-Ono K, Ono M, Yokoyama R, Nishitani K, Ishii T, Iwai H *et al.* 2014. XTH20 and XTH19 regulated by ANAC071 under auxin flow are involved in cell proliferation in incised *Arabidopsis* inflorescence stems. *The Plant Journal* 80: 604–614.

Qiu J-L, Fiil BK, Petersen K, Nielsen HB, Botanga CJ, Thorgrimsen S, Palma K, Suarez-Rodriguez MC, Sandbech-Clausen S, Lichota J *et al.* 2008. *Arabidopsis* MAP kinase 4 regulates gene expression through transcription factor release in the nucleus. *EMBO Journal* 27: 2214–2221.

Rajniak J, Barco B, Clay NK, Sattely ES. 2015. A new cyanogenic metabolite in *Arabidopsis* required for inducible pathogen defense. *Nature* 525: 376–379.

Ramirez-Parra E, Perianez-Rodriguez J, Navarro-Neila S, Gude I, Moreno-Risueno MA, del Pozo JC. 2017. The transcription factor OBP4 controls root growth and promotes callus formation. *New Phytologist* 213: 1787–1801.

Rennie EA, Hansen SF, Baidoo EEK, Hadi MZ, Keasling JD, Scheller HV. 2012. Three members of the *Arabidopsis* glycosyltransferase family 8 are xylan glucuronosyltransferases. *Plant Physiology* 159: 1408–1417.

Reymond P, Weber H, Damond M, Farmer EE. 2000. Differential gene expression in response to mechanical wounding and insect feeding in *Arabidopsis. The Plant Cell* 12: 707–720.

Rymen B, Kawamura A, Lambolez A, Inagaki S, Takebayashi A, Iwase A, Sakamoto Y, Sako K, Favero DS, Ikeuchi M *et al.* 2019. Histone acetylation orchestrates wound-induced transcriptional activation and cellular reprogramming in *Arabidopsis. Communications Biology* 2: 404.

Sarkar AK, Luijten M, Miyashima S, Lenhard M, Hashimoto T, Nakajima K, Scheres B, Heidstra R, Laux T. 2007. Conserved factors regulate signalling in *Arabidopsis thaliana* shoot and root stem cell organizers. *Nature* 446: 811–814.

Sato M, Mitra RM, Coller J, Wang D, Spivey NW, Dewdney J, Denoux C, Glazebrook J, Katagiri F. 2007. A high-performance, small-scale microarray for expression profiling of many samples in *Arabidopsis*-pathogen studies. *The Plant Journal* 49: 565–577.

Savatin DV, Gramegna G, Modesti V, Cervone F. 2014. Wounding in the plant tissue: the defense of a dangerous passage. *Frontiers in Plant Science* 5: 470.

Song JT, Lu H, McDowell JM, Greenberg JT. 2004. A key role for ALD1 in activation of local and systemic defenses in *Arabidopsis. The Plant Journal* 40: 200–212.

Soyano T, Thitamadee S, Machida Y, Chua NH. 2008. *ASYMMETRIC LEAVES2-LIKE19*/ *LATERAL ORGAN BOUNDARIES DOMAIN 30* and *ASL20*/ *LBD18* regulate tracheary element differentiation in *Arabidopsis. The Plant Cell* 20: 3359–3373.

Stobbe H, Shumitt U, Eckstein D, Dujesiefken D. 2002. Developmental stages and fine structure of surface callus formed after debarking of living lime trees (*Tilia* sp.). *Annals of Botany* 89: 773–782.

Stone SL, Kwong LW, Yee KM, Pelletier J, Lepiniec L, Fischer RL, Goldberg RB, Harada JJ. 2001. LEAFY COTYLEDON2 encodes a B3 domain transcription factor that induces embryo development. *Proceedings of the National Academy of Sciences, USA* 98: 11806–11811.

Storey JD, Tibshirani R. 2003. Statistical significance for genomewide studies. *Proceedings of the National Academy of Sciences, USA* 100: 9440–9445.

Su YH, Zhao XY, Liu YB, Zhang CL, O'Neill SD, Zhang XS. 2009. Auxin-induced WUS expression is essential for embryonic stem cell renewal during somatic embryogenesis in Arabidopsis. *Plant Journal* 59: 448–460.

Toyota M, Spencer D, Sawai-Toyota S, Jiaqi W, Zhang T, Koo AJ, Howe GA, Gilroy S. 2018. Glutamate triggers long-distance, calcium-based plant defense signaling. *Science* 361: 1112–1115.

Tucker MR, Lou H, Aubert MK, Wilkinson LG, Little A, Houston K, Pinto SC, Shirley NJ. 2018. Exploring the role of cell wall-related genes and polysaccharides during plant development. *Plants* 7: 42.

Valvekens D, Montagu MV, Van Lijsebettens M. 1988. *Agrobacterium tumefaciens-mediated* transformation of *Arabidopsis thaliana* root explants by using kanamycin selection. *Proceedings of the National Academy of Sciences, USA* 85: 5536–5540.

Van Lith-Vroom ML, Gottenbos JJ, Karstens WKH. 1960. General appearance, growth pattern, and anatomical structure of crown-gall tissue of *Nicotiana tabacum* L. grown in vitro on culture media containing glucose or soluble starch as a carbon source. *Acta Botanica Neerlandica* 9: 275–285.

Walker-Simmons M, Hollander-Czytko H, Andersen JK, Ryan CA. 1984. Wound signals in plants: a systemic plant wound signal alters plasma membrane integrity. *Proceedings of the National Academy of Sciences, USA* 81: 3737–3741.

Wang D, Amornsiripanitch N, Dong X. 2006. A genomic approach to identify regulatory nodes in the transcriptional network of systemic acquired resistance in plants. *PLoS Pathogens* 2: 1042–1050.

Wang Y, Schuck S, Wu J, Yang P, Doring AC, Zeier J, Tsuda K. 2018. A MPK3/6-WRKY33-ALD1-pipecolic acid regulatory loop contributes to systemic acquired resistance. *The Plant Cell* 30: 2480–2494.

White PR. 1939. Potentially unlimited growth of excised plant callus in an artificial nutrient. *American Journal of Botany* 26: 59–64.

Xu L, Huang H. 2014. Genetic and epigenetic controls of plant regeneration. *Current Topics in Developmental Biology* 108: 1–33.

Yoshida K, Sakamoto S, Kawai T, Kobayashi Y, Sato K, Ichinose Y, Yaoi K, Akiyoshi-Endo M, Sato H, Takamizo T *et al.* 2013. Engineering the *Oryza sativa* cell wall with rice NAC transcription factors regulating secondary wall formation. *Frontiers in Plant Science* 4: 383.

Zhang G, Zhao F, Chen L, Pan Yu, Sun L, Bao N, Zhang T, Cui C-X, Qiu Z, Zhang Y *et al.* 2019. Jasmonate-mediated wound signalling promotes plant regeneration. *Nature Plants* 5: 491–497.

Zhang T-Q, Lian H, Zhou C-M, Xu L, Jiao Y, Wang J-W. 2017. A two-step model for *de novo* activation of *WUSCHEL* during plant shoot regeneration. *The Plant Cell* 29: 1073–1087.

Zhou W, Lozano-Torres JL, Blilou I, Zhang X, Zhai Q, Smant G, Li C, Scheres B. 2019. A jasmonate signaling network activates root stem cells and promotes regeneration. *Cell* 177: 942–956.

Supporting Information

Additional Supporting Information may be found online in the Supporting Information section at the end of the article.

Fig. S1 Transcriptional changes after *WIND1* induction.

Fig. S2 RAP2.6 does not regulate callus formation at wound sites.

Fig. S3 WIND1 promotes xylem differentiation.

Fig. S4 Flagellin treatment upregulates *WIND1* expression.

Table S1 Genes upregulated in *XVE:WIND1* seedlings.

Table S2 Genes downregulated in *XVE:WIND1* seedlings.

Table S3 Heat-map representation of WIND1-induced transcriptional changes for genes, other than transcriptional regulators, implicated in vascular development.

Table S4 Heat-map representation of WIND1-induced transcriptional changes for genes, other than transcriptional regulators, implicated in pathogen response.

Table S5 Oligonucleotides used in this study.

Please note: Wiley Blackwell are not responsible for the content or functionality of any Supporting Information supplied by the authors. Any queries (other than missing material) should be directed to the *New Phytologist* Central Office.

About *New Phytologist*

- *New Phytologist* is an electronic (online-only) journal owned by the New Phytologist Foundation, a **not-for-profit organization** dedicated to the promotion of plant science, facilitating projects from symposia to free access for our Tansley reviews and Tansley insights.

- Regular papers, Letters, Viewpoints, Research reviews, Rapid reports and both Modelling/Theory and Methods papers are encouraged. We are committed to rapid processing, from online submission through to publication 'as ready' via *Early View* – our average time to decision is <26 days. There are **no page or colour charges** and a PDF version will be provided for each article.

- The journal is available online at Wiley Online Library. Visit **www.newphytologist.com** to search the articles and register for table of contents email alerts.

- If you have any questions, do get in touch with Central Office (np-centraloffice@lancaster.ac.uk) or, if it is more convenient, our USA Office (np-usaoffice@lancaster.ac.uk)

- For submission instructions, subscription and all the latest information visit **www.newphytologist.com**